Centro de Investigación y de Estudios Avanzados
del
Instituto Politécnico Nacional

DEPARTAMENTO DE FÍSICA

# Nanolistones de grafeno con terminaciones zigzag en campos magnéticos

**Tesis que presenta**

**Luis Joel Hernández Martínez**

para obtener el Grado de

Maestro en Ciencias

en la Especialidad de

Física

Director de tesis: **Dr. Alonso Contreras Astorga**

Ciudad de México Febrero, 2021

**CENTRO DE INVESTIGACION Y DE ESTUDIOS AVANZADOS DEL INSTITUTO POLITECNICO NACIONAL**

PHYSICS DEPARTMENT

# "Zigzag graphene nanoribbons in magnetic fields"

**Thesis submitted by**

**Luis Joel Hernández Martínez**

In order to obtain the

Master of Science

degree, speciality in

Physics

Supervisor: **Dr. Alonso Contreras Astorga**

Mexico City February, 2021.

# Agradecimientos

*Al* Dr. Alonso Contreras Astorga *por su apoyo y permitirme participar en este proyecto.*

*Gracias al* CINVESTAV *campus Zacatenco y al Programa de Becas Nacionales* CONACyT *por apoyar este trabajo, así como el apoyo parcial del proyecto* FORDECYT-PRONACES/61533/2020.

*Gracias a los sinodales* Dr. David José Fernández Cabrera *y* Dr. Alfredo Raya Montaño por su asesoría y consejos.

*Dedicado a mi madre* Esperanza *por el apoyo que me ha dado en todos estos años. Sin ella este trabajo no sería posible.*

# Contents

*Titulo de la tesis:*
**Nanolistones de grafeno con terminaciones zigzag en campos magnéticos**

*Autor:* Lic. Luis Joel Hernández Martínez

*Sinodales:* Dr. David José Fernández Cabrera.
Dr. Alfredo Raya Montaño

*Asesor de Tesis:* Dr. Alonso Contreras Astorga

*Resumen:*

Usando la mecánica cuántica supersimétrica de primer orden en nanolistones de grafeno con terminaciones zigzag sin campos magnéticos, construimos su Hamiltoniano de Dirac y el correspondiente espinor. Estudiamos las componentes del espinor, la ecuación de Schrödinger que satisface cada componente y su relación descrita por la mecánica cuántica supersimétrica. Aplicamos condiciones de frontera a las componentes del espinor para terminaciones zigzag y obtenemos soluciones para nanolistones de grafeno en campos magnéticos no uniformes. Además, implementamos la mecánica cuántica supersimétrica de primer orden una segunda vez a la ecuación de Schrödinger que satisface la componente superior del espinor y obtenemos una nueva familia de Hamiltonianos de Dirac para nanolistones de grafeno en un campo magnético cuyos espinores también cumplen las condiciones de frontera zigzag. El rango de valores para los parámetros introducidos por el algoritmo supersimétrico, donde los campos magnéticos y las soluciones son regulares, también fue estudiado.

*Title:*
**Zigzag graphene nanoribbons in magnetic fields**

*Author:* Lic. Luis Joel Hernández Martínez

*Abstract:*

Using the first-order supersymmetric quantum mechanics on graphene nanoribbons with zigzag edges without magnetic fields, we construct their Dirac Hamiltonian and the corresponding spinor. We study the spinor components, the Schrödinger equation that each component satisfies and their relationship described by supersymmetric quantum mechanics. We apply boundary conditions for zigzag edges to the spinor components and obtain solutions for graphene nanoribbons in non-uniform magnetic fields. Moreover, we implement the first-order supersymmetric quantum mechanics a second time to the Schrödinger equation satisfied by the upper spinor component and we obtain a new family of Dirac Hamiltonians for graphene nanoribbons in a magnetic field whose spinors also fulfill the zigzag boundary conditions. The range of values for the parameters introduced by the supersymmetric algorithm, where the magnetic fields and the solutions are regular, was as well studied.

# Introduction

Graphene is a flat hexagonal structure made of carbon atoms. It is one of the many allotropes of carbon as graphite, carbon nanotubes, fullerenes, etc. Its electronic structure was described for first time in 1947 [1], but it was until 2004 that it was found experimentally by Novoselov et al. [2], who received the Nobel Prize in Physics 2010 for that discovery [3]. The possibility of using graphene for multiple applications, such as for thermal control of electronic devices [4] or applications in electronics to produce smaller and flexible devices [5, 6] has generated great interest for this material.

In particular we study graphene nanoribbons, thin graphene sheets that can be classified into armchair and zigzag edges. These names describe the type of structure that the carbon atoms form at the edge of the graphene sheet. We start from solutions to the Dirac equation describing the behavior of electrons around the so-called *Dirac points* for zigzag graphene nanoribbons without magnetic field, and then we use supersymmetric quantum mechanic to obtain solutions to the Dirac equation for zigzag graphene nanoribbons with external magnetic fields.

It is worth noting that supersymmetric quantum mechanics, or SUSY, is a technique that allows us to use the eigenfunctions and energy spectrum of a known Hamiltonian $\hat{H}_0$ to find the eigenfunctions of another Hamiltonian $\hat{H}_1$ which conserve the energy spectrum, except perhaps by the ground state $\epsilon_0$ [7, 8, 9, 10].

The organization of this thesis is as follows. In Chapter 1, we will review the properties of a single-layer graphene and the importance of the Dirac

points. In Section 1.2 we will introduce the Dirac Hamiltonian $\hat{H}_D$ that describes the behavior of electrons near the Dirac points, and the appropriate boundary conditions for graphene nanoribbons with zigzag edges without magnetic field. In Section 1.3 we will show how the Dirac Hamiltonian for zigzag graphene nanoribbons is related to a Schrödinger equation.

In Chapter 2 we will give an introduction to supersymmetric quantum mechanics. In Section 2.2 we will show how to apply the first-order SUSY to a stationary Schrödinger equation, and we will discuss the situations when the supersymmetric technique generates regular potentials.

In Chapter 3 we will obtain several families of Dirac Hamiltonians for a nanoribbon in magnetic fields and we will find the spinors that solve the corresponding eigenvalue equation with zigzag boundary conditions. In Section 3.1 we start from the Schrödinger equation for one of the spinor components and use the first-order SUSY to obtain the expression for the Dirac Hamiltonian describing the zigzag graphene nanoribbons with magnetic field. In Section 3.2 we will use the solutions of Section 3.1 and the first-order supersymmetric quantum mechanics, to obtain a new Schrödinger equation for zigzag graphene nanoribbons with magnetic field. We will use again the first-order SUSY to obtain the expression for the new Dirac Hamiltonians for graphene nanoribbons that satisfy the zigzag boundary conditions.

Chapter 1

# Graphene

Graphene is an allotrope of carbon that consists of a single layer of atoms in a two-dimensional hexagonal lattice. P. R. Wallace in 1947 was the first one who described the band structure of graphene using the tight binding approximation [1]. However, first experimental realization of graphene was reported until 2004 by A. K. Geim and K. S. Novoselov [2] and in 2010 they received the Nobel Prize in Physics for the experimental discovery of graphene [3]. In the words of The Royal Swedish Academy of Science, they won the Prize

> *for groundbreaking experiments regarding the two-dimensional material graphene.*
>
> *(The Royal Swedish Academy of Sciences, 2010)*

Some characteristics of graphene are:

- It has beneficial properties for electronic applications like interface materials for thermal control of electronic device. The thermal conductivity of graphene is $10^3\,\mathrm{W\ m^{-1}K^{-1}}$ at room temperature [4].
- Its elastic properties make it the strongest material ever measured [11]. Its Young modulus is $\sim 10^{12}$ Pa.
- Graphene is a gapless semiconductor. In contrast, 2D semiconductors have bandgaps $> 1$ eV [12]. The minimun conductivity of graphene is

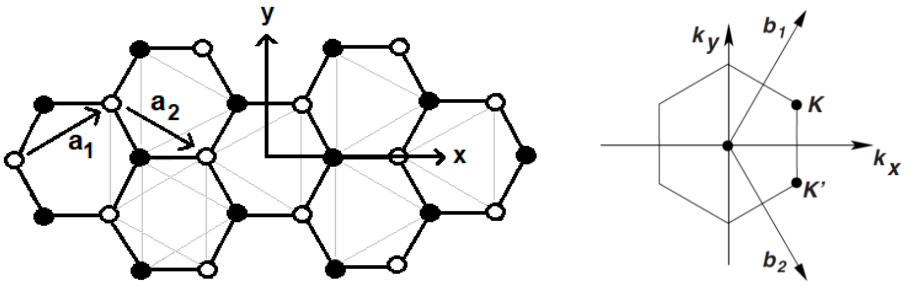


(a) Lattice of graphene (b) Reciprocal lattice

**Figure 1.1.** (a) Lattice of graphene. Graphene has two interpenetrating triangular lattices, the black or lattice A and the white or lattice B. (b) Reciprocal lattice of graphene. The points **K** and **K′** are the Dirac points.

between $2\,e^2/h - 12\,e^2/h$ [13] and the carrier mobility reaches $\sim 7\times10^4$ $\mathrm{cm}^2/\mathrm{v\,s}$ in transistors with different organic solvents [14].

Regarding its structure, graphene has two interpenetrating triangular lattices. In Figure 1.1 (a) we represented both lattices, one with black carbon atoms (lattice A) and the other with white atoms (lattice B). Each carbon atom is surrounded by three carbon atoms from the other lattice. Any point in the graphene lattice can be reached using the two lattice vectors

$$\mathbf{a}_1 = \frac{a}{2}\left(3,\,\sqrt{3}\right), \qquad \mathbf{a}_2 = \frac{a}{2}\left(3,\,-\sqrt{3}\right),$$

where $|\mathbf{a}_1| = |\mathbf{a}_2| = \sqrt{3}\,a = 0.246$ nm, with $a = 0.142$ nm being the carbon-carbon distance. Using the relation $\mathbf{a}_i\cdot\mathbf{b}_j = 2\pi\,\delta_{i\,j}$ we can define the reciprocal lattice vectors

$$\mathbf{b}_1 = \frac{2\pi}{3a}\left(1,\,\sqrt{3}\right), \qquad \mathbf{b}_2 = \frac{2\pi}{3a}\left(1,\,-\sqrt{3}\right).$$

Figure 1.1 (b) shows the points **K** and **K′** of the reciprocal lattice of graphene, where the valence and the conduction bands meet. These are known as Dirac points. Since both bands meet at those points, graphene is an excellent conductor [15].

The electronic properties of graphene are studied within the tight-binding approach. This formalism predicts that the energy bands are given by the

equation,

$$\epsilon_{\pm}(\mathbf{k}) = \pm t \sqrt{3 + 2\cos\left(\sqrt{3}k_y a\right) + 4\cos\left(\frac{\sqrt{3}}{2}k_y a\right)\,\cos\left(\frac{3}{2}k_x a\right)},$$

where the constant $t$ is the nearest-neighbor hopping energy ($t \approx 2.8$ eV), the plus sign applies to the conduction band and the minus sign to the valence band [16]. A characteristic of the energy bands is that $\epsilon_{\pm}(\mathbf{K}) = \epsilon_{\pm}(\mathbf{K}') = 0$, i.e., $\epsilon_{\pm}$ is zero at the Dirac points

$$\mathbf{K} = \left(\frac{2\pi}{3a}, \frac{2\pi}{3\sqrt{3}a}\right), \qquad \mathbf{K}' = \left(\frac{2\pi}{3a}, -\frac{2\pi}{3\sqrt{3}a}\right).$$

Near the Dirac points, where $\mathbf{k} = \mathbf{K} + \delta\mathbf{k}$, we have

$$\epsilon_{\pm} \approx \pm v_f |\mathbf{k}|,$$

where $v_f = \frac{3\,t\,a}{2} \approx 9.06 \times 10^5$ m/s is the Fermi velocity.

Using a nearest-neighbor tight-binding model and the $\mathbf{k}\cdot\mathbf{P}$ approximation, we obtain the equation that the electrons obey close to the Dirac points [17],

$$-\,i\,v_f\,\boldsymbol{\sigma}\cdot\nabla\boldsymbol{\psi}(\mathbf{r}) = E\,\boldsymbol{\psi}(\mathbf{r}), \tag{1.1}$$

where the spinor $\boldsymbol{\psi}(\mathbf{r})$ has two entries, $\boldsymbol{\sigma} = (\sigma_x, \sigma_y)$ and $\sigma_{x,y}$ are the Pauli matrices

$$\sigma_x = \begin{pmatrix} 0 & 1 \\ 1 & 0 \end{pmatrix}, \qquad \sigma_y = \begin{pmatrix} 0 & -i \\ i & 0 \end{pmatrix}, \qquad \sigma_z = \begin{pmatrix} 1 & 0 \\ 0 & -1 \end{pmatrix}. \tag{1.2}$$

Equation (1.1) resembles the time-independent relatisvistic Dirac equation,

$$c\,(-i\boldsymbol{\sigma}\cdot\nabla + \sigma_z m)\,\boldsymbol{\Psi} = E\,\boldsymbol{\Psi},$$

with $m = 0$ and $c \to v_f$. For this and other reasons some authors say that, for low energies and near the Dirac points, the electrons of graphene obey a Dirac equation with vanishing rest mass [15, 17].

## 1.1 Carbon nanotubes and graphene nanoribbons

Two very important carbon nanomaterials are the so called carbon nanotubes (CNT) and graphene nanoribbons (GNR). CNT can be single-walled (SWCNT) or multiwalled (MWCNT). The SWCNT is a single graphene sheet rolled into a tube, whereas the MWCNT is a carbon nanotube with several concentric shells of rolled graphene sheets [18].

The SWCNT was discovered by two different research groups in 1993, by Iijima and Ichihashi [19] and Bethune et al. [20]. They are classified into three groups according to the chiral vector $\mathbf{C}_h$, a vector that crosses the SWCNT perpendicular to the tube axis,

$$\mathbf{C}_h = n\,\mathbf{a}_1 + m\,\mathbf{a}_2,$$

where $n$ and $m$ are integers. This chiral vector defines all the possible ways of rolling-up a graphene sheet:

- Zigzag, where $n \neq 0$ and $m = 0$.
- Armchair, where $n = m$.
- Chiral, where $n, m \neq 0$.

Figure 1.2 shows the chiral vector that gives place to an armchair carbon nanotube.

Graphene nanoribbons are strips of graphene with thin widths. Similar to nanotubes, the GNR are classified into armchair and zigzag. These names refer to the orientation of the carbon atoms on the edge of the graphene sheet, as can be seen in Figure 1.3.

CNT and GNR are obtained from single-layer graphene, but their band structure is different. For example, CNT is metallic when $n - m = 3\,\nu$, with $\nu$ an integer [21, 18]. Instead, zigzag GNRs are always metallic while the armchair GNRs are metallic when the number $N$ of carbon atoms across the width is $N = 3\,\nu - 1$ and semiconductors when $N = 3\,\nu$ or $N = 3\,\nu + 1$ [18].

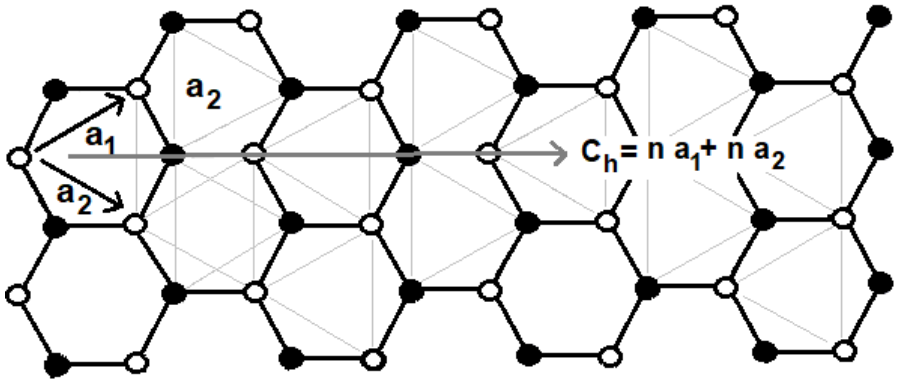


**Figure 1.2.** Chiral vector for an armchair SWCNT. It shows how to roll graphene to form an armchair carbon nanotube.

## 1.2 Zigzag boundary conditions for graphene nanoribbons

Brey and Fertig published two important articles in 2006 [22, 23]. In both articles they used the Dirac equation to study the electronic states of graphene nanoribbons and gave special boundary conditions for zigzag and armchair graphene nanoribbons of width $L$ and infinite length without external magnetic field as well as in a uniform magnetic field. They found that, except for very thin GNR, their results were quantitatively similar to the one of the tight binding calculations. In what follow we will develop their results for zigzag GNR following to Castro Neto et al. [16].

For low-energy states and near the Dirac points, we can write the Dirac equation (1.1) for the points $\mathbf{K}$ as

$$\hat{H}_{\mathbf{K}}\,\boldsymbol{\psi}_{\mathbf{K}}(\mathbf{r}) = v_f \begin{pmatrix} 0 & -i\,\partial_x - \partial_y \\ -i\partial_x + \partial_y & 0 \end{pmatrix} \boldsymbol{\psi}_{\mathbf{K}}(\mathbf{r}) = \epsilon\,\boldsymbol{\psi}_{\mathbf{K}}(\mathbf{r})\,, \qquad (1.3)$$

and for the points $\mathbf{K}'$ as

$$\hat{H}_{\mathbf{K}'}\,\boldsymbol{\psi}_{\mathbf{K}'}(\mathbf{r}) = v_f \begin{pmatrix} 0 & -i\,\partial_x + \partial_y \\ -i\partial_x - \partial_y & 0 \end{pmatrix} \boldsymbol{\psi}_{\mathbf{K}'}(\mathbf{r}) = \epsilon\,\boldsymbol{\psi}_{\mathbf{K}'}(\mathbf{r})\,. \qquad (1.4)$$

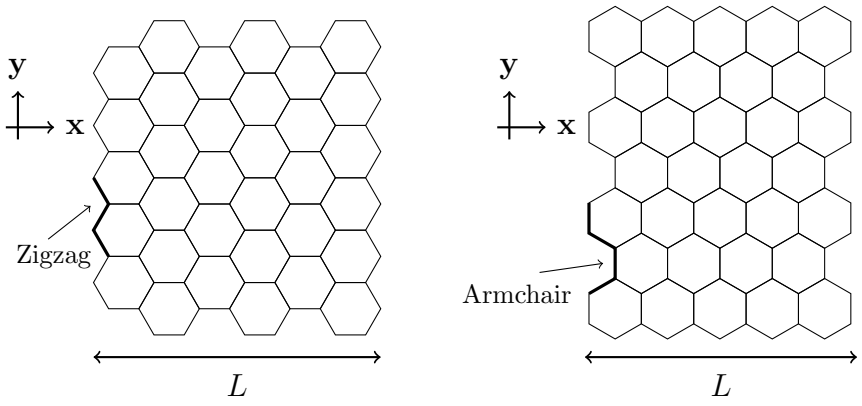


(a) Zigzag GNR. (b) Armchair GNR.

**Figure 1.3.** (a) Zigzag and (b) armchair graphene nanoribbons. $L$ is the width of the nanoribbon with infinite length.

Recall now that graphene has two interpenetrating triangular lattices, the lattices A and B from Figure 1.1 (a). The wave function (real space) for the lattice A is given by [16]

$$\Psi_A(\mathbf{r}) = e^{i\mathbf{K}\cdot\mathbf{r}}\psi_A(\mathbf{r}) + e^{i\mathbf{K}'\cdot\mathbf{r}}\psi'_A(\mathbf{r}),$$

and for the lattice B by

$$\Psi_B(\mathbf{r}) = e^{i\mathbf{K}\cdot\mathbf{r}}\psi_B(\mathbf{r}) + e^{i\mathbf{K}'\cdot\mathbf{r}}\psi'_B(\mathbf{r}).$$

The functions $\psi_A(\mathbf{r})$ and $\psi_B(\mathbf{r})$ are the components of the spinor $\boldsymbol{\psi}_{\mathbf{K}}(\mathbf{r})$ while $\psi'_A(\mathbf{r})$ and $\psi'_B(\mathbf{r})$ are the components of $\boldsymbol{\psi}_{\mathbf{K}'}(\mathbf{r})$,

$$\boldsymbol{\psi}_{\mathbf{K}}(\mathbf{r}) = \begin{pmatrix} \psi_A(\mathbf{r}) \\ \psi_B(\mathbf{r}) \end{pmatrix}, \qquad \boldsymbol{\psi}_{\mathbf{K}'}(\mathbf{r}) = \begin{pmatrix} \psi'_A(\mathbf{r}) \\ \psi'_B(\mathbf{r}) \end{pmatrix}.$$

We assume that our zigzag GNR is on the $XY$ plane, it has finite width $L$, infinite lenght and the zigzag edges are on the lines $x = 0$ and $x = L$ respectively, as Figure 1.3 (a) shows. The translational symmetry in the $Y$ direction, along the zigzag edge, guarantees that the spinor $\boldsymbol{\psi}_{\mathbf{K}}$ or $\boldsymbol{\psi}_{\mathbf{K}'}$ can

be written as,

$$\boldsymbol{\psi}_{\mathbf{K}}\,(x,y) = e^{i\,k_y\,y}\begin{pmatrix}\phi_A\,(x)\\ \phi_B\,(x)\end{pmatrix}, \qquad \boldsymbol{\psi}_{\mathbf{K}'}\,(x,y) = e^{i\,k_y\,y}\begin{pmatrix}\phi^{'}_A\,(x)\\ \phi^{'}_B\,(x)\end{pmatrix}.$$

with $k_y$ a real constant. The boundary conditions for GNR at the edges of the nanoribbon, located at $x = 0$ and $x = L$, are,

$$\Psi_A\,(0,y) = 0, \qquad \Psi_B\,(L,y) = 0,$$

these two conditions give us that,

$$e^{i\,\mathbf{K}\cdot\mathbf{r}}\,e^{i\,k_y\,y}\phi_A(0)\; + e^{i\,\mathbf{K}'\cdot\mathbf{r}}e^{i\,k_y\,y}\phi^{'}_A(0) = 0,$$

$$e^{i\,\mathbf{K}\cdot\mathbf{r}}\,e^{i\,k_y\,y}\phi_B(L)\; + e^{i\,\mathbf{K}'\cdot\mathbf{r}}e^{i\,k_y\,y}\phi^{'}_B(L) = 0.$$

Both conditions are satisfied when,

$$\phi_A(0) = \phi^{'}_A(0) = \phi_B(L) = \phi^{'}_B(L) = 0. \tag{1.5}$$

Conditions (1.5) are called zigzag boundary conditions and they will be used constantly in this work.

The Dirac Hamiltonians $\hat{H}_{\mathbf{K}}$ and $\hat{H}_{\mathbf{K}'}$ of equations (1.3) and (1.4) applied to their respective spinors generate the system of equations

$$\begin{pmatrix}0 & -i\partial_x - i\,k_y\\ -i\partial_x + i\,k_y & 0\end{pmatrix}\begin{pmatrix}\phi_A(x)\\ \phi_B(x)\end{pmatrix} = \frac{\epsilon}{v_f}\begin{pmatrix}\phi_A(x)\\ \phi_B(x)\end{pmatrix}, \tag{1.6}$$

$$\begin{pmatrix}0 & -i\partial_x + i\,k_y\\ -i\partial_x - i\,k_y & 0\end{pmatrix}\begin{pmatrix}\phi^{'}_A(x)\\ \phi^{'}_B(x)\end{pmatrix} = \frac{\epsilon}{v_f}\begin{pmatrix}\phi^{'}_A(x)\\ \phi^{'}_B(x)\end{pmatrix}. \tag{1.7}$$

Both systems of equations can be written in terms of Schrödinger Hamiltonians if we multiply them by the energy $\bar{\epsilon} = \epsilon/v_f$, namely, if

$$\hat{H}_0 = \begin{pmatrix}0 & -i\partial_x - i\,k_y\\ -i\partial_x + i\,k_y & 0\end{pmatrix}, \qquad \Phi(x) = \begin{pmatrix}\phi_A(x)\\ \phi_B(x)\end{pmatrix}, \tag{1.8}$$

then,

$$\hat{H}_0\,\{\bar{\epsilon}\,\Phi(x)\} = \bar{\epsilon}^2\,\Phi(x) \quad \rightarrow \quad \hat{H}_0\left\{\hat{H}_0\,\Phi(x)\right\} = \bar{\epsilon}^2\,\Phi(x),$$

where,

$$\hat{H}_0^2 = \hat{H}_0\,\hat{H}_0 = \begin{pmatrix} -\partial_x^2 + k_y^2 & 0 \\ 0 & -\partial_x^2 + k_y^2 \end{pmatrix}.$$

The procedure for the components $\phi_A^{'}(x)$ and $\phi_B^{'}(x)$ is analogous. Thus, we have to solve the same equation for the components of both spinors,

$$-\frac{d^2\,\phi_\mu^{(')}}{dx^2} + k_y^2\,\phi_\mu^{(')}(x) = \bar{\epsilon}^2\,\phi_\mu^{(')}(x), \qquad \mu = A, B. \tag{1.9}$$

We use the superscript $(')$ to indicate that the equation (1.9) is the same for $\phi_\mu(x)$ and $\phi_\mu^{'}(x)$. The general solution of (1.9) is

$$\phi_\mu^{(')}(x) = \alpha\,e^{z\,x} + \beta\,e^{-z\,x}, \tag{1.10}$$

where $z^2 = k_y^2 - \bar{\epsilon}^2$.

Another property of this system is that the Hamiltonians $\hat{H}_{\mathbf{K}}$ and $\hat{H}_{\mathbf{K}'}$ are related through the Pauli matrix $\sigma_x$, defined in (1.2). The relationship between them is given by

$$\hat{H}_{\mathbf{K}'} = \sigma_x\,\hat{H}_{\mathbf{K}}\,\sigma_x. \tag{1.11}$$

Thus, we can obtain the spinor $\boldsymbol{\psi}_{\mathbf{K}'}$ from the spinor $\boldsymbol{\psi}_{\mathbf{K}}$. The proof begins by multiplying equation (1.3) by $\sigma_x$

$$\hat{H}_{\mathbf{K}}\,\boldsymbol{\psi}_{\mathbf{K}}(\mathbf{r}) = \epsilon\,\boldsymbol{\psi}_{\mathbf{K}}(\mathbf{r}) \quad \rightarrow \quad \sigma_x\hat{H}_{\mathbf{K}}\,\boldsymbol{\psi}_{\mathbf{K}}(\mathbf{r}) = \epsilon\,\sigma_x\,\boldsymbol{\psi}_{\mathbf{K}}(\mathbf{r}),$$

we can use the properties of the Pauli matrices $\sigma_x^2 = I$, where $I$ is the identity matrix. Then,

$$\sigma_x\hat{H}_{\mathbf{K}}\,\sigma_x\,(\sigma_x\,\boldsymbol{\psi}_{\mathbf{K}}(\mathbf{r})) = \epsilon\,(\sigma_x\,\boldsymbol{\psi}_{\mathbf{K}}(\mathbf{r})) \quad \rightarrow \quad \hat{H}_{\mathbf{K}'}\,(\sigma_x\,\boldsymbol{\psi}_{\mathbf{K}}(\mathbf{r})) = \epsilon\,(\sigma_x\,\boldsymbol{\psi}_{\mathbf{K}}(\mathbf{r}))\,.$$

Therefore, $\boldsymbol{\psi}_{\mathbf{K}'}(\mathbf{r}) = \sigma_x\,\boldsymbol{\psi}_{\mathbf{K}}(\mathbf{r})$. Consequently, we will work only with the spinor $\boldsymbol{\psi}_{\mathbf{K}}$.

To fulfill the zigzag boundary conditions (1.5) we must take $\beta = -\alpha$, we arrive at

$$\phi_A(x) = \alpha\left(e^{z\,x} - e^{-z\,x}\right).$$

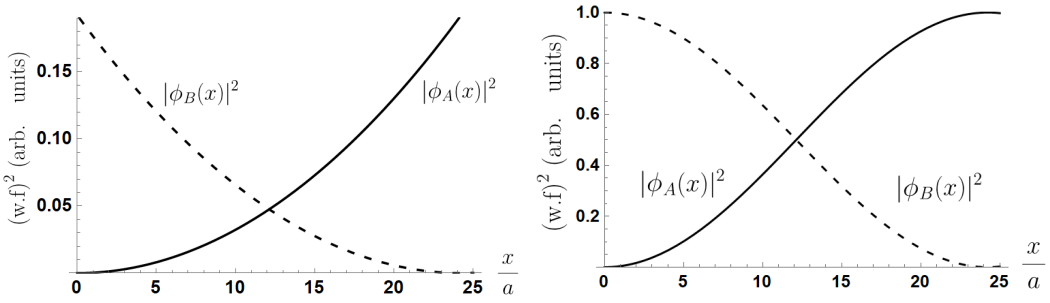


(a) $k_y = \frac{4\pi}{300\,a}$. (b) $k_y = 0$.

**Figure 1.4.** Modulus square of the lower and upper spinor components for the ground state energy with $k_y$ being a real number. (a) Case with $k_y \neq 0$ and $z = z_1 = 8.971 \times 10^{-3}$, the spinor components are a linear combination of exponential functions. (b) Case with $k_y = 0$ and $z = i\,k_0 = i\,\pi/2$, the spinor components are a linear combination of trigonometric functions. The width of the nanoribbon is chosen as $L = 14\sqrt{3}\,a$.

Analyzing the lower component of the Dirac equation $\hat{H}_0\,\Phi(x) = \bar{\epsilon}\,\Phi(x)$ we obtain

$$\phi_B(x) = \frac{1}{\bar{\epsilon}}\left(-i\,\partial_x + ik_y\right)\phi_A(x) = -\frac{i\,\alpha}{\bar{\epsilon}}\left[(z-k_y)e^{z\,x} + (z+k_y)e^{-z\,x}\right],$$

when we apply the boundary condition $\phi_B(L) = 0$ it gives us the transcendental equation

$$e^{-2\,z\,L} = \frac{k_y - z}{k_y + z}. \tag{1.12}$$

The solutions of this equation generate a list of real numbers $z$ that are related to the energy spectrum. Moreover, let us note that if $z = i\,k_n$ we obtain another important transcendental equation,

$$\tan k_n\,L = \frac{k_n}{k_y}. \tag{1.13}$$

### 1.2.1 Examples

In their first article [22], Brey and Fertig showed two examples. The first example is for $z$ being a real number, this case corresponds to the surface

states. The energy of these states is $\bar{\epsilon} = \pm\sqrt{k_y^2 - z^2}$, and the spinor components $\phi_A(x)$ and $\phi_B(x)$ that solve the system of equations (1.6) are

$$\phi_A(x) = \alpha \left(e^{z\,x} - e^{-z\,x}\right), \tag{1.14}$$

$$\phi_B(x) = -\frac{i\,\alpha}{\bar{\epsilon}} \left[(z - k_y)e^{z\,x} + (z + k_y)e^{-z\,x}\right]. \tag{1.15}$$

For this case they choose $k_y = \frac{4\pi}{300\,a}$. The transcendental equation (1.12) has three solutions for $z$: $z_0 = 0$ and $z_{1,-1} = \pm\,8.971 \times 10^{-3}$. The solution $z_0$ is the trivial one because $\phi_A(x) \equiv$ cte. The solutions $z_1$ and $z_{-1}$ are similar and lead to the same energy. In Figure 1.4 (a) we can see the modulus square of the spinor components for $z_1$.

The second example is for $z$ being a pure imaginary number. Each solution $k_n$ generates two confined states with energies $\bar{\epsilon} = \pm\sqrt{k_y^2 + k_n^2}$ and spinor components

$$\phi_A(x) = 2\,i\alpha\,\sin k_n\,x, \tag{1.16}$$

$$\phi_B(x) = \frac{2\,\alpha}{\bar{\epsilon}}\left(k_n\,\cos k_n\,x - k_y \sin k_n\,x\right). \tag{1.17}$$

Furthermore, in this case they choose $k_y = 0$. The transcendental equation (1.13) has the following solutions for $k_n$:

$$k_n = \frac{2\,n+1}{2}\pi, \qquad n = 0, 1, 2, 3, \cdots$$

The energies are given by $\bar{\epsilon}_n = \pm\,k_n$. If we choose $n = 0$ we obtain the ground state eigenfunction, which can be seen in Figure 1.4 (b).

## 1.3 Relation between Schrödinger and Dirac equations

The low-energy behavior of massless Dirac electrons in graphene, around the Dirac points, under a magnetic field $\mathbf{B} = \nabla \times \mathbf{A}$ is described by the Dirac-Weyl equation [24],

$$\hat{H}_D \boldsymbol{\psi}\,(x, y) = v_f\,\boldsymbol{\sigma} \cdot [-i\,\nabla + \mathbf{A}]\,\boldsymbol{\psi}\,(x, y) = E\,\boldsymbol{\psi}\,(x, y)\,, \tag{1.18}$$

where the magnetic field is perpendicular to the graphene layer. In (1.18) $\boldsymbol{\sigma} = (\sigma_x, \sigma_y)$ and we have taken $c = e = \hbar = 1$. We can obtain equation (1.18) from equation (1.1) by using

$$-i\,\nabla \quad \rightarrow \quad -i\,\nabla + \mathbf{A}.$$

This change is known as minimal coupling [25] or Peierls substitution [23].

In Section 1.2 we assumed that the graphene sheet was on the $XY$ plane. Now, we will assume that the vector potential is given by $\mathbf{A}\,(x) = A_y(x)\,\hat{e}_y$. This choice is known as *Landau gauge*, which produces the magnetic field

$$\mathbf{B}(x) = \frac{d\,A_y(x)}{dx}\,\hat{e}_z \tag{1.19}$$

pointing along $z$ direction. The most general option would be to take $\mathbf{A} = A_x(y)\,\hat{e}_x + A_y(x)\,\hat{e}_y$, which is called the Coulomb gauge. Also, vector potentials of the form $\mathbf{A}' = A_y(x)\,\hat{e}_y + \nabla\eta$, where $\nabla\eta$ is a constant, generate magnetic fields parallel to the $z$ direction.

After Peierls substitution in equation (1.18), the eigenvalue equation $\hat{H}_D\,\boldsymbol{\psi} = E\boldsymbol{\psi}$ can be written as

$$v_f\left[-i\sigma_x\frac{\partial}{\partial x} + \sigma_y\left(-i\,\frac{\partial}{\partial y} + A_y(x)\right)\right]\boldsymbol{\psi}\,(x,y) = E\,\boldsymbol{\psi}\,(x,y)\,.$$

In Section 1.2 we also saw that $\boldsymbol{\psi}\,(x,y) = e^{i\,k_y\,y}\,\Phi(x)$. Then,

$$\hat{H}_D\,\Phi(x) = v_f\left[-i\sigma_x\frac{d}{dx} + \sigma_y\,\omega(x)\right]\Phi(x) = E\,\Phi(x), \tag{1.20}$$

where $\omega(x) = k_y + A_y(x)$, with $k_y$ being a real constant. The product $\hat{H}_D\,\hat{H}_D$ produces a pair of Schrödinger equations:

$$\hat{H}_D^2\,\Phi(x) = v_f^2\begin{pmatrix} -\frac{d^2}{dx^2} + V_+\,(x) & 0 \\ 0 & -\frac{d^2}{dx^2} + V_-\,(x) \end{pmatrix}\Phi(x) = E^2\,\Phi(x),$$

where

$$V_\pm\,(x) = \omega^2(x) \pm \frac{d\,\omega\,(x)}{dx}, \qquad \Phi(x) = \begin{pmatrix} \phi_A(x) \\ \phi_B(x) \end{pmatrix}. \tag{1.21}$$

This result is similar to that seen in equation (1.9), but with $A_y(x) = 0$. In order to have the same notation, now we change the variable $E/v_f$ to $\bar{\epsilon} = \epsilon/v_f$. Thus, we have the following two Schrödinger equations:

$$\hat{H}_+ \, \phi_A \, (x) = \left( -\frac{d^2}{dx^2} + V_+ \, (x) \right) \, \phi_A \, (x) = \bar{\epsilon}^2 \, \phi_A \, (x), \tag{1.22}$$

$$\hat{H}_- \, \phi_B \, (x) = \left( -\frac{d^2}{dx^2} + V_- \, (x) \right) \phi_B \, (x) = \bar{\epsilon}^2 \, \phi_B \, (x). \tag{1.23}$$

In summary, we have started with the Dirac-Weyl equation (1.20) and obtained two Schrödinger equations. The inverse process is also possible, starting with a Schrödinger equation to obtain the Dirac equation (1.20). We can do it by defining $\omega(x) = \nu'(x)/\nu(x)$ and replacing it in the definition of $V_+(x)$ , equation (1.21), which is called Riccati equation. Thus we obtain:

$$-\frac{d^2\nu(x)}{dx^2} + V_+(x)\,\nu(x) = 0. \tag{1.24}$$

After solving the Schrödinger equation (1.24) we will get the expressions for $\omega(x)$ and then the Dirac equation (1.20). This process is similar if we use $V_-(x)$ of equation (1.21) with the replacement $\omega(x) \to -\nu'(x)/\nu(x)$. In forthcoming Sections we will work exclusively with the procedure described for $V_+(x)$.

The components for the spinor $\Phi(x)$ are obtained through the pair of coupled differential equations (1.20):

$$-\,i\,\left( \frac{d\,\phi_B(x)}{dx} + \omega(x)\;\phi_B(x) \right) = \bar{\epsilon}\;\phi_A(x), \tag{1.25}$$

$$-\,i\,\left( \frac{d\,\phi_A(x)}{dx} - \omega(x)\;\phi_A(x) \right) = \bar{\epsilon}\;\phi_B(x). \tag{1.26}$$

We can solve this system of equations as follows. If we first solve equation (1.22) for the component $\phi_A(x)$, we can obtain the component $\phi_B(x)$ using (1.26),

$$\phi_B(x) = -\frac{i}{\bar{\epsilon}} \left( \frac{d\,\phi_A(x)}{dx} - \omega(x)\;\phi_A(x) \right). \tag{1.27}$$

This procedure we will follow in the future. The other alternative is to solve (1.23) for the component $\phi_B(x)$. The upper spinor component $\phi_A(x)$ can be

obtained through equation (1.25) because

$$\phi_A(x) = -\frac{i}{\bar{\epsilon}}\left(\frac{d\,\phi_B(x)}{dx} + \omega(x)\ \phi_B(x)\right). \tag{1.28}$$

This is the appropriate procedure for the case when $\omega(x) = -\nu'(x)/\nu(x)$.

The energy spectrum of the Dirac Hamiltonian is obtained from the energy spectrum of the Schrödinger Hamiltonian. While we were studying how to obtain the Hamiltonians $\hat{H}_+$ of (1.22) and $\hat{H}_-$ of (1.23) from the Hamiltonian $\hat{H}_D$, we found that if $\epsilon_D$ represents the spectrum of $\hat{H}_D$ and $\epsilon_H$ represents the spectrum of $\hat{H}_\pm$, the relationship between them is given by

$$\epsilon_D = \pm\sqrt{\epsilon_H}.$$

Chapter 2

# Supersymmetric Quantum Mechanics

Supersymmetric quantum mechanics is a technique that allows to manipulate the energy spectrum of a Hamiltonian, or, for special potentials, it can be used to find the solution for new Hamiltonians.

Historically, the origin of this technique is the factorization method, introduced by Dirac in 1935 in the second edition of his quantum mechanics book [26], where he solved algebraically the spectral problem for the one-dimensional quantum harmonic oscillator. A few years later, in 1951, Infeld and Hull published an extensive work [27] identifying several potentials and systems, that were not limited to the harmonic oscillator, where the factorization method can be applied [28]. In 1984 Mielnik generalized the factorization method through the harmonic oscillator Hamiltonian [29]. His work opened new ways of solving potentials in quantum mechanics by showing that if the factorization operators were exchanged a new Hamiltonian could be obtained [30]. More information on the subject and the supersymmetric quantum mechanics can be found in the following books and reviews [7, 31, 8, 9]

One way to introduce supersymmetric quantum mechanics is by introducing the operators $Q^+$ and $Q^-$ [31]:

$$Q^+ = \begin{pmatrix} 0 & L^+ \\ 0 & 0 \end{pmatrix}, \qquad Q^- = \begin{pmatrix} 0 & 0 \\ L^- & 0 \end{pmatrix},$$

with $L^\pm$ being differential operators of $k$-th order. The operators $Q^\pm$ commute

with the Hamiltonian $\hat{H}$,

$$[Q^{\pm},\, \hat{H}] = 0, \qquad \hat{H} = \begin{pmatrix} L^+\, L^- & 0 \\ 0 & L^-\, L^+ \end{pmatrix}.$$

The operators $L^{\pm}$ are related to two Schrödinger Hamiltonians $\hat{H}_0$ and $\hat{H}_1$ in the following way

$$L^+\, L^- = \prod_{i=1}^{k} \left(\hat{H}_1 - \epsilon_i\right), \qquad L^-\, L^+ = \prod_{i=1}^{k} \left(\hat{H}_0 - \epsilon_i\right),$$

where $\epsilon_i$ are eigenvalues of $\hat{H}_0$ whose meaning we will see later. Multiplying the operators $Q^+$ and $Q^-$ we obtain:

$$Q^+Q^- = \begin{pmatrix} L^+\, L^- & 0 \\ 0 & 0 \end{pmatrix}, \qquad Q^-Q^+ = \begin{pmatrix} 0 & 0 \\ 0 & L^-\, L^+ \end{pmatrix}.$$

Notice that:

$$\{Q^-,\, Q^+\} = Q^-Q^+ + Q^+Q^- = \hat{H}.$$

The Hamiltonian $\hat{H}$ is called supersymmetric Hamiltonian, while $Q^+$ and $Q^-$ are the supercharges.

If we want to intertwine the Hamiltonians $\hat{H}_0$ and $\hat{H}_1$, whose potentials are $V_{0,1}(x)$ respectively, we need to select $k$ formal eigenfunctions $u_i$ of one of them, we choose $\hat{H}_0$, for different eigenvalues $\epsilon_i$,

$$\hat{H}_0\, u_i(x) = \epsilon_i\, u_i(x), \qquad i = 1, 2, \cdots, k.$$

The formal eigenfunctions $u_i(x)$ are called seed solutions, and the corresponding $\epsilon_i$ factorization energies. If the Hamiltonians are of the form

$$\hat{H}_0 = -\frac{d^2}{dx^2} + V_0(x), \qquad \hat{H}_1 = -\frac{d^2}{dx^2} + V_1(x),$$

then the relationship between the two potentials is given by,

$$V_1(x) = V_0(x) - \frac{d^2\, \ln\left[W(u_1, \cdots, u_k)\right]}{dx^2},$$

with $W(u_1, \cdots, u_k)$ being the Wronskian of the seed solutions $u_i(x)$. There is also a relationship involving the Hamiltonians $\hat{H}_0$, $\hat{H}_1$ and the operators $L^{\pm}$:

$$\hat{H}_0 L^- = L^- \hat{H}_1, \qquad \hat{H}_1 L^+ = L^+ \hat{H}_0.$$

The last intertwining relation tells us how the eigenfunctions of both Hamiltonians are related. If the eigenfunctions of $\hat{H}_1$ are $\phi_n^{(1)}(x)$ and the ones of $\hat{H}_0$ are $\phi_n^{(0)}(x)$, it turns out that

$$\phi_n^{(1)}(x) = \frac{L^+ \phi_n^{(0)}(x)}{\sqrt{(E_n - \epsilon_1) \cdots (E_n - \epsilon_k)}}.$$

The eigenvalues of $\hat{H}_0$ and $\hat{H}_1$ are also related, but it does not mean that they are equal. Each time that an eigenvalue $E_n$ of $\hat{H}_0$ is equal to a factorization energy, that $\epsilon_1$ could not be part of the spectrum of $\hat{H}_1$.

In what follows, we will work exclusively with the first-order supersymmetric quantum mechanics, i.e., we will make $k = 1$.

## 2.1 First-order supersymmetric quantum mechanics

In the first-order supersymmetric quantum mechanics (or 1-SUSY) the differential intertwining operators are of first-order, and take the form:

$$L^+ = -\frac{d}{dx} + W(x), \qquad L^- = \frac{d}{dx} + W(x), \tag{2.1}$$

where $W(x)$ is called superpotential.

The 1-SUSY only needs a seed solution $u(x)$ with a factorization energy $\epsilon$ such that $\hat{H}_0\, u(x) = \epsilon\, u(x)$. The intertwined Hamiltonians $\hat{H}_0$ and $\hat{H}_1$ are related to the operators $L^{\pm}$ as follows,

$$\hat{H}_0 = L^- L^+ + \epsilon, \qquad \hat{H}_1 = L^+ L^- + \epsilon.$$

About the energy spectrum of $\hat{H}_0$ and $\hat{H}_1$ we will have three cases [32]: the spectrum of $\hat{H}_1$ is the same as the spectrum of $\hat{H}_0$ except by the ground state; the spectrum of $\hat{H}_1$ contains the complete spectrum of $\hat{H}_0$ plus the new

energy level $\epsilon$; $\hat{H}_0$ and $\hat{H}_1$ have exactly the same energy spectrum.

For each of these cases the sets of eigenfunctions and eigenvalues of $\hat{H}_1$ become:

- Deleting of the ground state of $\hat{H}_0$: this means that $\epsilon = E_0$ and $u(x) = \phi_0^{(0)}(x)$. Thus, the eigenfunctions and eigenvalues of $\hat{H}_1$ are:

$$\phi_{n-1}^{(1)}(x) = \frac{L^+\,\phi_n^{(0)}(x)}{\sqrt{E_n - E_0}}, \qquad E_{n-1}^{(1)} = E_n^{(0)}, \qquad n = 1, 2, 3, \cdots$$

- Creating a new level: this means that $\epsilon < E_0$ and the seed solution $u(x)$ is nodeless in the $x$-domain of the potential. The sets of eigenfunctions and eigenvalues of $\hat{H}_1$ will be:

$$\phi_\epsilon^{(1)} \propto \frac{1}{u(x)}, \quad \phi_n^{(1)}(x) = \frac{L^+\phi_n^{(0)}(x)}{\sqrt{E_n - \epsilon}},\ n = 0, 1, 2, \cdots$$

$$\mathrm{Sp}(\hat{H}_1) = \{\epsilon, E_n^{(0)},\ n = 0, 1, 2, \cdots\}.$$

- Isospectral transformation: it appears for $\epsilon < E_0$ and $u(x)$ having a node at one of the ends of the $x$-domain of the potential. As $\phi_\epsilon \propto 1/u(x)$ diverges at such a node, then $\phi_\epsilon$ is not square-integrable. Thus, the eigenfunctions and eigenvalues of $\hat{H}_1$ are,

$$\phi_n^{(1)} = \frac{L^+\,\phi_n^{(0)}}{\sqrt{E_n - \epsilon}}, \qquad E_n^{(1)} = E_n^{(0)}, \qquad n = 0, 1, 2, \cdots$$

## 2.2 Intertwining operators for zigzag graphene nanoribbons

In Section 1.3 we wrote a series of relations that allow us to obtain a Dirac Hamiltonian from a Schrödinger equation and the components of its spinor. In equations (1.27) and (1.28) we can see the following operators to appear,

$$L^+ = -\frac{d}{dx} + \omega(x), \qquad L^- = \frac{d}{dx} + \omega(x). \tag{2.2}$$

Thus, we can write equations (1.27) and (1.28) in the way:

$$\phi_B(x) = \frac{i\,L^+\,\phi_A(x)}{\bar{\epsilon}}, \qquad \phi_A(x) = -\frac{i\,L^-\phi_B(x)}{\bar{\epsilon}}.$$

Therefore, the Schrödinger equations for $\hat{H}_+$ in (1.22) and $\hat{H}_-$ in (1.23) can be factorized by the operators, $L^+$ and $L^-$. Then, we can express these Schrödinger Hamiltonians as follows,

$$\hat{H}_+ = L^- L^+, \qquad \hat{H}_- = L^+ L^-. \tag{2.3}$$

If we expand these products, using the definitions in (2.2), we get that

$$\hat{H}_+ = -\frac{d^2}{dx^2} + \omega'(x) + \omega^2(x),$$

$$\hat{H}_- = -\frac{d^2}{dx^2} - \omega'(x) + \omega^2(x).$$

These expressions appear in equations (1.22) and (1.23). Therefore, $\omega(x)$ is a superpotential and the Hamiltonians $\hat{H}_+$ and $\hat{H}_-$ are supersimmetric partners, which satisfy the intertwining relations,

$$\hat{H}_+ L^- = L^- \hat{H}_-, \qquad \hat{H}_- L^+ = L^+ \hat{H}_+. \tag{2.4}$$

Note that the Hamiltonian $\hat{H}_+$ can generate different partner Hamiltonians $\hat{H}_-$ when we shift the energy and potential $V_+$ by a real constant $\xi$,

$$\hat{H}_+ \, \phi_A(x) = \left( -\frac{d^2}{dx^2} + \{V_+(x) - \xi\} \right) \phi_A(x) = \left\{ \bar{\epsilon}^2 - \xi \right\} \phi_A(x),$$

Now, equation (1.24) for $\nu(x)$ becomes,

$$-\frac{d^2\nu(x)}{dx^2} + V_+(x)\,\nu(x) = \xi\,\nu(x). \tag{2.5}$$

Thus, adding a constant energy $\xi$ does not only modify the partner Hamiltonian $\hat{H}_-$, but it also changes the superpotential $\omega(x)$, the operators $L^\pm$ and the eigenfunctions of $\hat{H}_-$. These changes generate new interesting solutions that we will explore in the next chapter.

Chapter 3

# Zigzag graphene nanoribbons under magnetic fields

In Chapter 1 we described the Dirac Hamiltonian and Schrödinger equation that the zigzag graphene nanoribbons must fulfill, as well as its associated boundary conditions. We developed the method to obtain a Dirac Hamiltonian starting from a Schrödinger equation and vice versa, as well as determining its spinor.

In Chapter 2 we developed the first-order supersymmetric quantum mechanics, or 1-SUSY. This technique allows us to obtain solutions of a Schrödinger equation from solutions of another Schrödinger equation, preserving the energy spectrum except by the ground state, which can change or be preserved.

In this Chapter we employ the solutions for zigzag graphene nanoribbons of Chapter 1 and apply the 1-SUSY technique to them. The goal will be to obtain new solutions to the Dirac Hamiltonian (1.20) with magnetic fields from the solutions that Brey and Fertig found for zigzag nanoribbons without magnetic fields. Examples of the use of supersymmetry to relate Dirac Hamiltonians with Schrödinger equations can be found in [33, 34, 35]. In the works [24, 25, 36, 37] the authors as well study the way of using supersymmetry for graphene under magnetic fields.

## 3.1 Zeroth SUSY transformation of a zigzag graphene nanoribbon

In Section (1.2) we derived the Schrödinger equation (1.9) that must fulfill the components $\phi_n^{(A)}(x)$ and $\phi_n^{(B)}(x)$ of the spinor $\Phi(x)$. Let us go back to that equation and add a zero in the way $\xi - \xi = 0$, with $\xi$ being a real constant. Thus we obtain the following Schrödinger equation

$$\hat{H}_0^2\,\phi_n^{(A)}(x) = \left(-\frac{d^2}{dx^2} + k_y'^2\right)\,\phi_n^{(A)}(x) = \bar{\epsilon}_n'^2\,\phi_n^{(A)}(x), \tag{3.1}$$

where

$$k_y'^2 = k_y^2 - \xi, \qquad \bar{\epsilon}_n'^2 = \bar{\epsilon}_n^2 - \xi, \qquad \bar{\epsilon}_n^2 = k_y^2 - z_n^2,$$

and $\phi_n^{(A)}(x)$ is the upper component of the spinor. As we can see, the constant $\xi$ shifts the potential and the energy levels.

In what follows, we will derive the Dirac equation $\hat{H}_D$ starting from the Schrödinger equation (3.1) using the procedure described in Section 1.3. We can distinguish two important cases, the first one where $z_n = \sqrt{k_y^2 - \bar{\epsilon}_n^2}$ is real for $k_y^2 > \bar{\epsilon}_n^2$ and the second one where $z_n$ is a pure imaginary number for $k_y^2 < \bar{\epsilon}_n^2$. In the first case, it is convenient to express $\phi_n^{(A)}(x)$ as

$$\phi_n^{(A)}(x) = A\,\sinh z_n\,x + B\,\cosh z_n\,x, \tag{3.2}$$

whereas in the second case $\phi_n^{(A)}(x)$ takes the form

$$\phi_n^{(A)}(x) = A\,\sin k_n\,x + B\,\cos k_n\,x. \tag{3.3}$$

We can use equation (1.27) to know the lower spinor component $\phi_n^{(B)}(x)$. When $z_n^2 > 0$ we have

$$\begin{aligned}\phi_n^{(B)}(x) = \;& \tfrac{i\,A}{\bar{\epsilon}'}\,\left[-z_n\,\cosh z_n\,x + \omega(x)\,\sinh z_n\,x\right] \\ & + \tfrac{i\,B}{\bar{\epsilon}'}\,\left[-z_n\,\sinh z_n\,x + \omega(x)\,\cosh z_n\,x\right],\end{aligned} \tag{3.4}$$

while for $z_n = i\,k_n$ we obtain

$$\begin{aligned}\phi_n^{(B)}(x) = \;& \tfrac{i\,A}{\bar{\epsilon}'}\,\left[-k_n\,\cos k_n\,x + \omega(x)\,\sin k_n\,x\right] \\ & + \tfrac{i\,B}{\bar{\epsilon}'}\,\left[k_n\,\sin k_n\,x + \omega(x)\,\cos k_n\,x\right].\end{aligned} \tag{3.5}$$

Now we need to know $\omega(x) = \nu'(x)/\nu(x)$, where $\nu(x)$ is the solution of the Schrödinger equation,

$$\left(-\frac{d^2}{dx^2} + k_y'^2\right)\nu(x) = 0 \qquad \text{or} \qquad \left(-\frac{d^2}{dx^2} + k_y^2\right)\nu(x) = \xi\,\nu(x).$$

Once again we have two solutions. For $k_y^2 - \xi > 0$ the solution is

$$\nu(x) = C\,\cosh\sqrt{k_y^2 - \xi}\,x + D\,\sinh\sqrt{k_y^2 - \xi}\,x.$$

We can rewrite it using a constant phase $\alpha$, where $C = \cosh\alpha$ and $D = \sinh\alpha$. We thus get

$$\nu(x) = \cosh\left(\sqrt{k_y^2 - \xi}\,x + \alpha\right). \tag{3.6}$$

Then, $\omega(x)$ is given by

$$\omega(x) = \sqrt{k_y^2 - \xi}\,\tanh\left(\sqrt{k_y^2 - \xi}\,x + \alpha\right). \tag{3.7}$$

The function $\omega(x)$ is necessary to find the expressions for the Dirac equation (1.20) and for the lower spinor component $\phi_n^{(B)}(x)$. The Dirac Hamiltonian in this case is

$$\hat{H}_D = v_f\left\{-i\sigma_x\frac{d}{dx} + \sigma_y\left[\sqrt{k_y^2 - \xi}\,\tanh\left(\sqrt{k_y^2 - \xi}\,x + \alpha\right)\right]\right\}. \tag{3.8}$$

The other solution arises for $k_y^2 - \xi < 0$,

$$\nu(x) = C\,\cos\sqrt{\xi - k_y^2}\,x + D\,\sin\sqrt{\xi - k_y^2}\,x.$$

We can also rewrite it using now the constants $C = \cos\alpha$ and $D = -\sin\alpha$. Then,

$$\nu(x) = \cos\left(\sqrt{\xi - k_y^2}\,x + \alpha\right). \tag{3.9}$$

In this case the function $\omega(x)$ and the Dirac Hamiltonian are, respectively,

$$\omega(x) = -\sqrt{\xi - k_y^2}\,\tan\left(\sqrt{\xi - k_y^2}\,x + \alpha\right), \tag{3.10}$$

$$\hat{H}_D = v_f\left\{-i\sigma_x\frac{d}{dx} - \sigma_y\left[\sqrt{\xi - k_y^2}\,\tan\left(\sqrt{\xi - k_y^2}\,x + \alpha\right)\right]\right\}. \tag{3.11}$$

Another important result related to the function $\omega(x)$ has to do with the magnetic field $\mathbf{B}(x)$. In Section 1.3 we saw that $\omega(x)$ is related to the vector potential $\mathbf{A} = A_y(x)\,\hat{e}_y$ through the expression,

$$\omega(x) = k_y + A_y(x).$$

Equation (1.19) tells us that the magnetic field is the derivative with respect to $x$ of $A_y(x)$ but, since $k_y$ is a constant, such a derivative coincides with the derivative with respect to $x$ of $\omega(x)$,

$$\mathbf{B}(x) = \frac{d\,\omega(x)}{dx}\,\hat{e}_z. \tag{3.12}$$

When $k_y^2 - \xi > 0$ the magnetic field is

$$\mathbf{B}\,(x) = \left(k_y^2 - \xi\right) \operatorname{sech}^2\left(\sqrt{k_y^2 - \xi}\,x + \alpha\right)\hat{e}_z, \tag{3.13}$$

while for $k_y^2 - \xi < 0$ it becomes

$$\mathbf{B}\,(x) = -\left(\xi - k_y^2\right) \sec^2\left(\sqrt{\xi - k_y^2}\,x + \alpha\right)\hat{e}_z. \tag{3.14}$$

These results are summarized in Table 3.2.

### 3.1.1 Zeros of the function $\nu(x)$.

In Chapter 2 (section 2.2) we saw that $\nu(x)$ is a seed solution associated to the parameter $\xi$ of equation (2.5) and the functions $\phi_n^{(B)}(x)$ can be interpreted as eigenfunctions of the corresponding partner Hamiltonian of the operator $\hat{H}_0^2$ in equation (3.1). In Section 2.1 three different cases were identified when $\nu(x)$ is a nodeless function in the $x$-domain or it has a node at one of the ends. Let us study now the two expressions for $\nu(x)$ that we found in this Chapter, equations (3.6) and (3.9), to determine the values that $\alpha$ and $\sqrt{k_y^2 - \xi}$ can have. The first case is for

$$\nu(x) = \cosh\left(\sqrt{k_y^2 - \xi}\,x + \alpha\right),$$

which is not null for all values of $x$ between $[0, 1]$. Thus, any value of $\xi$, $k_y$ and $\alpha$ are valid whenever $k_y^2 - \xi > 0$. If $k_y^2 - \xi < 0$ it turns out that:

$$\nu(x) = \cos\left(\sqrt{\xi - k_y^2}\,x + \alpha\right).$$

| Case | $\alpha$ | $\sqrt{\lvert k_y^2 - \xi \rvert}$ |
|---|---|---|
| $k_y^2 - \xi > 0$ | All | All |
| $k_y^2 - \xi < 0$ | $\left(-\frac{\pi}{2},\, \frac{\pi}{2}\right)$ | $\left[-\frac{\pi}{2} - \alpha,\, \frac{\pi}{2} - \alpha\right]$ |
| | $0$ or $\pm\pi$ | $\left[-\frac{\pi}{2},\, \frac{\pi}{2}\right]$ |
| | $\pm\frac{\pi}{2}$ | $(-\pi, 0)$ or $(0, \pi)$ |
| | $\left(\frac{\pi}{2},\, \pi\right)$ | $\left[\frac{\pi}{2} - \alpha,\, \frac{3\pi}{2} - \alpha\right]$ |
| | $\left(-\pi,\, -\frac{\pi}{2}\right)$ | $\left[-\frac{3\pi}{2} - \alpha,\, -\frac{\pi}{2} - \alpha\right]$ |

**Table 3.1.** Allowed values of $\alpha$ and $\sqrt{|k_y^2 - \xi|}$ for $x \in [0, 1]$. These values define a function $\nu(x)$ without nodes or with a node at one of the ends of the $x$-domain. If $\pi$ is added or subtracted to $\alpha$ the condition for $\sqrt{|k_y^2 - \xi|}$ does not change.

The cosine function vanishes when its argument takes the values,

$$\frac{2\,n+1}{2}\,\pi, \qquad n = 0, 1, 2, \cdots$$

In Table 3.1 we show the values of $\alpha$ and $\sqrt{|k_y^2 - \xi|}$ that define $\nu(x)$ as a function without nodes in the closed interval $[0, 1]$ or with a node at one of the ends.

### 3.1.2 Zigzag boundary conditions

In Section 1.2 we saw that the upper and lower components of the spinor $\Phi(x)$ for zigzag graphene nanoribbons must satisfy the boundary conditions

$$\phi_n^{(A)}(0) = 0, \qquad \phi_n^{(B)}(1) = 0.$$

We have normalized the boundary conditions (1.5) with the change of variable $x \to x/L$.

In Section 3.1 we presented general expressions, without considering the proper boundary conditions. Since the upper spinor component $\phi_n^{(A)}$ must vanish at $x = 0$, see equations (3.2) and (3.3), we have that $B = 0$. Therefore, when $z_n = \sqrt{k_y^2 - \bar{\epsilon}_n^2}$ is a real number we have:

$$\phi_n^{(A)}(x) = A \, \sinh z_n \, x, \tag{3.15}$$

$$\phi_n^{(B)}(x) = \frac{i \, A}{\bar{\epsilon}_n'} \, [ -z_n \, \cosh z_n \, x + \omega(x) \, \sinh z_n \, x \, ]. \tag{3.16}$$

Instead, when $z_n = i \, k_n$ is a pure imaginary number it is obtained:

$$\phi_n^{(A)}(x) = A \, \sin k_n \, x, \tag{3.17}$$

$$\phi_n^{(B)}(x) = \frac{i \, A}{\bar{\epsilon}_n'} \, [ -k_n \, \cos k_n \, x + \omega(x) \, \sin k_n \, x \, ]. \tag{3.18}$$

Using now the second boundary condition, $\phi_n^{(B)}(1) = 0$, we obtain the following transcendental equation when $z_n$ is a real number,

$$\coth \, z_n = \frac{\omega(1)}{z_n}.$$

The hyperbolic cotangent function can be written in terms of the exponential function in the way

$$\coth \, z_n = \frac{1 + e^{-2 \, z_n}}{1 - e^{-2 \, z_n}}.$$

Thus, when $k_y^2 - \xi > 0$ it is obtained

$$e^{-2 \, z_n} = \frac{-z_n + \sqrt{k_y^2 - \xi} \, \tanh \left( \sqrt{k_y^2 - \xi} + \alpha \right)}{z_n + \sqrt{k_y^2 - \xi} \, \tanh \left( \sqrt{k_y^2 - \xi} + \alpha \right)}, \tag{3.19}$$

but if $k_y^2 - \xi < 0$ it turns out that

$$e^{-2 \, z_n} = -\frac{z_n + \sqrt{\xi - k_y^2} \, \tan \left( \sqrt{\xi - k_y^2} + \alpha \right)}{z_n - \sqrt{\xi - k_y^2} \, \tan \left( \sqrt{\xi - k_y^2} + \alpha \right)}. \tag{3.20}$$

If the variable $z_n$ is imaginary, that is $z_n = i \, k_n$, the exponential function is written in terms of trigonometric functions. Thus, for $k_y^2 - \xi > 0$ we have

$$\tan \, k_n = \frac{k_n}{\sqrt{k_y^2 - \xi} \, \tanh \left( \sqrt{k_y^2 - \xi} + \alpha \right)}, \tag{3.21}$$

while for $k_y^2 - \xi < 0$ it is obtained:

$$\tan\, k_n = -\frac{k_n}{\sqrt{\xi - k_y^2}\, \tan\left(\sqrt{\xi - k_y^2} + \alpha\right)}. \tag{3.22}$$

These results are summarized in Table 3.2.

### 3.1.3 Example

Now, let us see an example using the parameters $\alpha = \pi$, $\xi = \frac{1}{4}\pi^2$ and $k_y = 0$. Since $k_y^2 - \xi = -\frac{1}{4}\pi^2$ is negative we must take,

$$\nu(x) = \cos\left(\sqrt{\xi - k_y^2}\, x + \pi\right),$$

$$\omega(x) = -\sqrt{\xi - k_y^2}\, \tan\left(\sqrt{\xi - k_y^2}\, x + \pi\right),$$

with $\sqrt{\xi - k_y^2} = \frac{\pi}{2}$, let us note that $\nu(x)$ have a node at $x = 1$. While the corresponding magnetic field is given by

$$\mathbf{B}(x) = -\left(\xi - k_y^2\right)\, \sec^2\left(\sqrt{\xi - k_y^2}\, x + \alpha\right)\, \hat{e}_z.$$

In Figure 3.4 (a) we show plots of the function $\omega(x)$ and the magnetic field $B(x)$.

The spinor components $\phi_n^{(A)}(x)$ and $\phi_n^{(B)}(x)$ are obtained by solving the transcendental equations for $z_n$ being a real number:

$$e^{-2\, z_n} = \zeta(z_n) = -\frac{z_n + \sqrt{\xi - k_y^2}\, \tan\left(\sqrt{\xi - k_y^2} + \alpha\right)}{z_n - \sqrt{\xi - k_y^2}\, \tan\left(\sqrt{\xi - k_y^2} + \alpha\right)},$$

and for $z_n = i\, k_n$:

$$\tan\, k_n = \kappa(k_n) = -\frac{k_n}{\sqrt{\xi - k_y^2}\, \tan\left(\sqrt{\xi - k_y^2} + \alpha\right)}.$$

The transcendental equation when $z_n$ is a real number give us the solution $z_n = 0$. We can see this if we rewrite the function $\zeta(z_n)$ as,

$$-\frac{z_n + \sqrt{\xi - k_y^2}\, \tan\left(\sqrt{\xi - k_y^2} + \alpha\right)}{z_n - \sqrt{\xi - k_y^2}\, \tan\left(\sqrt{\xi - k_y^2} + \alpha\right)} = -\frac{z_n\, \left[\sqrt{\xi - k_y^2}\, \tan\left(\sqrt{\xi - k_y^2} + \alpha\right)\right]^{-1} + 1}{z_n\, \left[\sqrt{\xi - k_y^2}\, \tan\left(\sqrt{\xi - k_y^2} + \alpha\right)\right]^{-1} - 1}.$$

| Function | $k_y^2-\xi>0$ | $k_y^2-\xi<0$ |
|---|---|---|
| $\nu(x)$ | $\cosh\left(\sqrt{k_y^2-\xi}\,x+\alpha\right)$ | $\cos\left(\sqrt{\xi-k_y^2}\,x+\alpha\right)$ |
| $\omega(x)$ | $\sqrt{k_y^2-\xi}\,\tanh\left(\sqrt{k_y^2-\xi}\,x+\alpha\right)$ | $-\sqrt{\xi-k_y^2}\tan\left(\sqrt{\xi-k_y^2}\,x+\alpha\right)$ |
| $\mathbf{B}(x)$ | $\left(k_y^2-\xi\right)\,\mathrm{sech}^2\left(\sqrt{k_y^2-\xi}\,x+\alpha\right)\,\hat{e}_z$ | $-\left(\xi-k_y^2\right)\,\sec^2\left(\sqrt{\xi-k_y^2}\,x+\alpha\right)\,\hat{e}_z$ |
| $z_n=\sqrt{k_y^2-\bar{\epsilon}_n^2}$ real | | |
| T.E. | $e^{-2\,z_n}=\frac{-z_n+\sqrt{k_y^2-\xi}\,\tanh\left(\sqrt{k_y^2-\xi}+\alpha\right)}{z_n+\sqrt{k_y^2-\xi}\,\tanh\left(\sqrt{k_y^2-\xi}+\alpha\right)}$ | $e^{-2\,z_n}=-\frac{z_n+\sqrt{\xi-k_y^2}\,\tan\left(\sqrt{\xi-k_y^2}+\alpha\right)}{z_n-\sqrt{\xi-k_y^2}\,\tan\left(\sqrt{\xi-k_y^2}+\alpha\right)}$ |
| $\phi_n^{(A)}(x)$ | $\sinh z_n\,x$ | |
| $\phi_n^{(B)}(x)$ | $\frac{i}{\sqrt{\bar{\epsilon}_n^2-\xi}}\left[-z_n\,\cosh z_n\,x+\omega(x)\sinh z_n\,x\right]$ | |
| $z_n=ik_n$ with $k_n=\sqrt{\bar{\epsilon}_n^2-k_y^2}$ | | |
| T.E. | $\tan\,k_n=\frac{k_n}{\sqrt{k_y^2-\xi}\,\tanh\left(\sqrt{k_y^2-\xi}+\alpha\right)}$ | $\tan\,k_n=-\frac{k_n}{\sqrt{\xi-k_y^2}\,\tan\left(\sqrt{\xi-k_y^2}+\alpha\right)}$ |
| $\phi_n^{(A)}(x)$ | $\sin k_n\,x$ | |
| $\phi_n^{(B)}(x)$ | $\frac{i}{\sqrt{\bar{\epsilon}_n^2-\xi}}\left[-k_n\,\cos k_n\,x+\omega(x)\sin k_n\,x\right]$ | |

**Table 3.2.** Expressions of the functions $\nu\,(x)$, $\omega\,(x)$, the magnetic field $\mathbf{B}\,(x)$ and the lower and upper spinor components $\phi_n^{(A)}(x)$ and $\phi_n^{(B)}(x)$ for different possible cases considering boundary conditions $\phi_n^{(A)}(0)=0$ and $\phi_n^{(B)}(1)=0$. T.E. means transcendental equation.

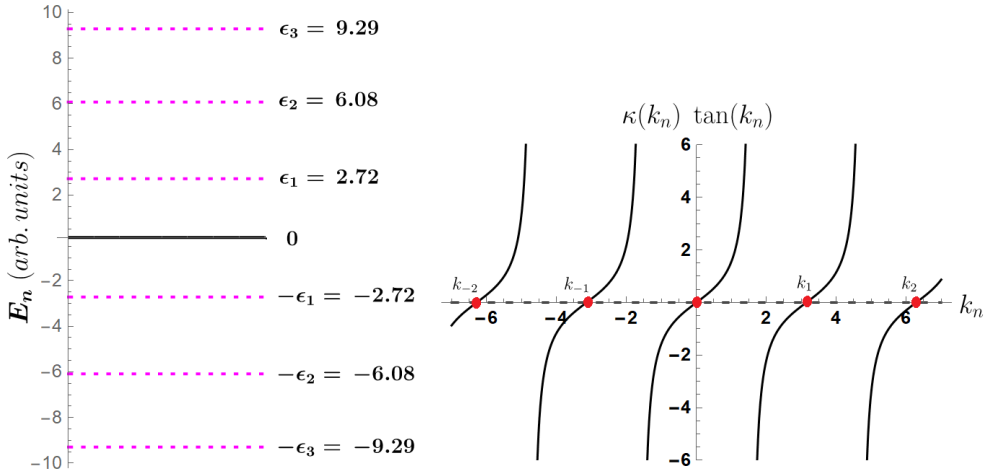


(a) Energy spectrum for $\hat{H}_D$.

(b) Solutions for $z_n = i\,k_n$.

**Figure 3.1.** Energy spectrum (left) and solutions of the transcendental equation for $z_n = i\,k_n$ (right). The points represent the allowed values of $k_n$. The values of the parameters used are $\alpha = \pi$, $\xi = \frac{\pi^2}{4}$ and $k_y = 0$.

Then, when $\sqrt{\xi - k_y^2} = \frac{\pi}{2}$ and $\alpha = \pi$ we get that

$$\sqrt{\xi - k_y^2} + \alpha \to \frac{3}{2}\pi, \quad \text{and} \quad \tan\left(\sqrt{\xi - k_y^2} + \alpha\right) \to \infty.$$

Thus, the transcendental equation becomes $e^{-2\,z_n} \to 1$, whose solution is $z_n = 0$. This solution is not useful because $\phi_n^{(A)}(x)$ will be identically zero and $\phi_n^{(B)}(x)$ will be a constant for any $x$ in $[0, 1]$.

When $z_n = i\,k_n$ the transcendental equation $\kappa(k_n)$ is a zero function, because $\tan\left(\sqrt{\xi - k_y^2} + \alpha\right) \to \infty$, and the intersections between $\kappa(k_n)$ and $\tan(k_n)$ arise at the multiples of $\pi$. Thus, we get that

$$k_n = n\,\pi, \qquad n = \pm 1,\, \pm 2,\, \pm 3,\, \ldots.$$

The energy spectrum of the Schrödinger Hamiltonian $\hat{H}_0^2$, defined in equation (3.1), is calculated from $\bar{\epsilon}_n'^2 = k_y^2 - z_n^2 - \xi$, which is given by

$$\bar{\epsilon}_n'^2 = \left(n^2 - \frac{1}{4}\right)\pi^2, \qquad n = \pm 1,\, \pm 2,\, \pm 3,\, \ldots$$

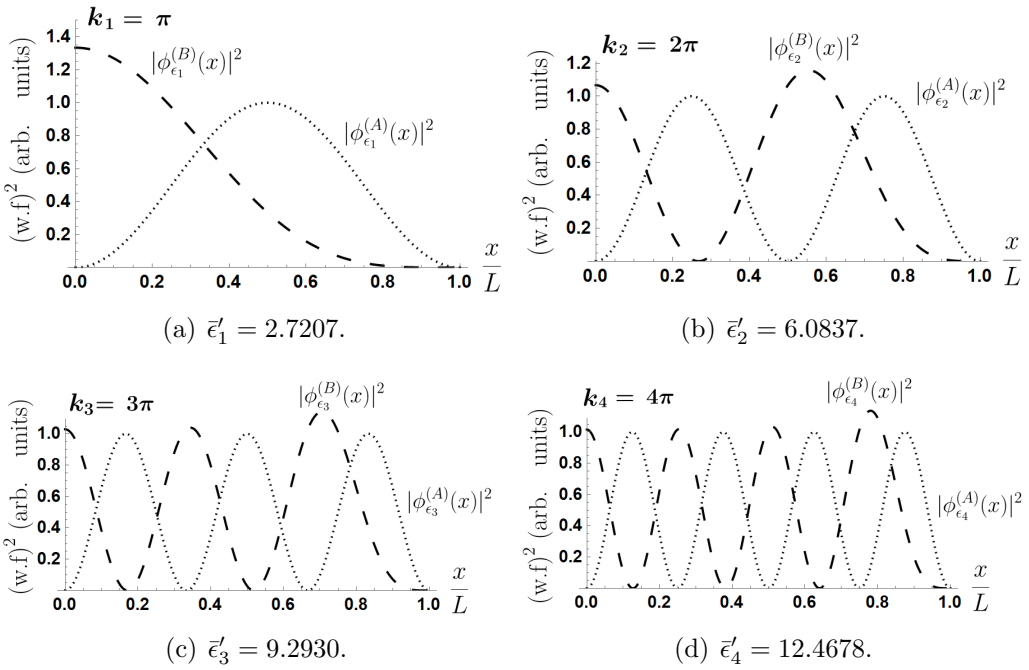


(a) $\bar{\epsilon}'_1 = 2.7207$. (b) $\bar{\epsilon}'_2 = 6.0837$.

(c) $\bar{\epsilon}'_3 = 9.2930$. (d) $\bar{\epsilon}'_4 = 12.4678$.

**Figure 3.2.** Modulus square of the entries of the normalized spinor with parameters $\alpha = \pi$, $\xi = \frac{\pi^2}{4}$ and $k_y = 0$ for the first four positive energies.

The energies $\bar{\epsilon}'^2_n$ are always positive, which means that $\xi < \bar{\epsilon}^2_n$, and the function $\nu(x)$ have a node at $x = 1$. Therefore, this case corresponds to an isospectral 1-SUSY transformation, see Section 2.1.

The energies of the Dirac Hamiltonian $\hat{H}_D$ are $\bar{\epsilon}'_n = \pm\sqrt{\bar{\epsilon}'^2_n}$. In Figure 3.1 (a) we show a plot of some energies of $\hat{H}_D$ while in Figure 3.1 (b) we can see the intersections between the functions $\kappa(k_n)$ and $\tan(k_n)$. The values of $z_n$ are represented by points.

Therefore, the spinor components $\phi^{(A)}_n(x)$ and $\phi^{(B)}_n(x)$ are given by

$$\phi^{(A)}_n(x) = A \sin k_n x,$$

$$\phi^{(B)}_n(x) = -\frac{i\,A}{\sqrt{\bar{\epsilon}^2_n - \xi}}\left[k_n \cos k_n x + \sqrt{\xi - k_y^2}\tan\left(\sqrt{\xi - k_y^2}\,x + \alpha\right)\sin k_n x\right],$$

where $A$ is a normalization constant. We find this constant using numerical

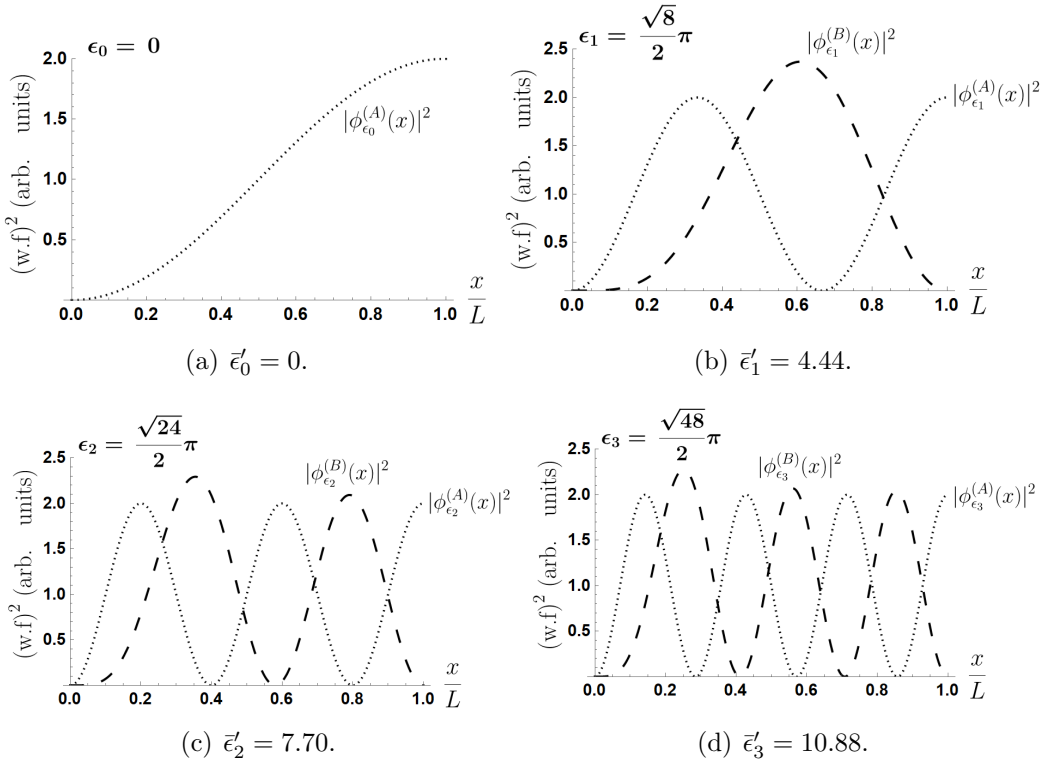


(a) $\bar{\epsilon}'_0 = 0$. (b) $\bar{\epsilon}'_1 = 4.44$.

(c) $\bar{\epsilon}'_2 = 7.70$. (d) $\bar{\epsilon}'_3 = 10.88$.

**Figure 3.3.** Modulus square of the components of the normalized spinor $\Phi(x)$ with parameters $\alpha = \frac{3}{2}\pi$ and $\sqrt{\xi - k_y^2} = \frac{1}{2}\pi$ for the first four positive energies. Note that this case can be also interpreted as a 1-SUSY transformation on the potential $V_0 = -\frac{1}{4}\pi^2$.

integration with the normalization condition,

$$\int_0^1 \left( |\phi_n^{(A)}(x)|^2 + |\phi_n^{(B)}(x)|^2 \right) dx = 1.$$

The functions $\phi_n^{(A)}(x)$ are similar to the eigenfunctions of a particle in an infinite potential well of length $L = 1$. This happens because the solutions to the transcendental equation become multiples of $\pi$, and therefore,

$$\phi_n^{(A)}(0) = \phi_n^{(A)}(1) = 0.$$

In Figure 3.2 we show plots of the modulus square of the spinor components for the first four positive energies, whose normalization constants are:

| | $k_1$ | $k_2$ | $k_3$ | $k_4$ |
|---|---|---|---|---|
| $A$ | 1.0 | 1.0 | 1.0 | 1.0 |

A second example emerges from the previous one if we make the following substitution in the function $\nu(x)$,

$$x \to x+1 \quad \to \quad \nu(x) = \cos\left(\frac{\pi}{2}\,x + \frac{3\,\pi}{2}\right).$$

Then, we can obtain another solution for the parameters $k_y^2 - \xi = -\frac{1}{4}\pi^2$ and $\alpha = \frac{3}{2}\pi$. Although we are shifting the variable $x$ in the seed solution, our interval of interest will remain $[0, 1]$.

The expression for $\omega(x)$ is given by

$$\omega(x) = -\frac{\pi}{2}\,\tan\left(\frac{\pi}{2}\,x + \frac{3\,\pi}{2}\right) = \frac{\pi}{2}\,\cot\left(\frac{\pi}{2}\,x\right).$$

The magnetic field has the same expression

$$\mathbf{B}(x) = -\left(\xi - k_y^2\right)\,\sec^2\left(\sqrt{\xi - k_y^2}\,x + \alpha\right)\,\hat{e}_z.$$

In Figure 3.4 (b) we show a plot of the magnetic field $B(x)$ for this example.

The transcendental equations that we have to solve are the same as in the previos example, but now the solutions obtained when $z_n = i\,k_n$ become

$$k_n = \frac{2n+1}{2}\pi, \qquad n = 0,\, \pm1,\, \pm2,\, \pm3,\, \ldots,$$

and the energies for the Schrödinger Hamiltonian $\hat{H}_0^2$ are given by,

$$\bar{\epsilon}_n'^2 = \left[\left(n + \frac{1}{2}\right)^2 - \frac{1}{4}\right]\pi^2, \qquad n = 0,\, \pm1,\, \pm2,\, \pm3,\, \ldots.$$

These expression for $\bar{\epsilon}_n'^2$ are similar to the previous example, but with the index change $n \to n+1/2$. Another difference is that the lowest value of $\bar{\epsilon}_n'^2$ is zero, which means that for $n = 0$ we get $\xi = \bar{\epsilon}_0^2$. Thus, this case corresponds to a 1-SUSY transformation that deletes the ground state energy of the $\hat{H}_0^2$

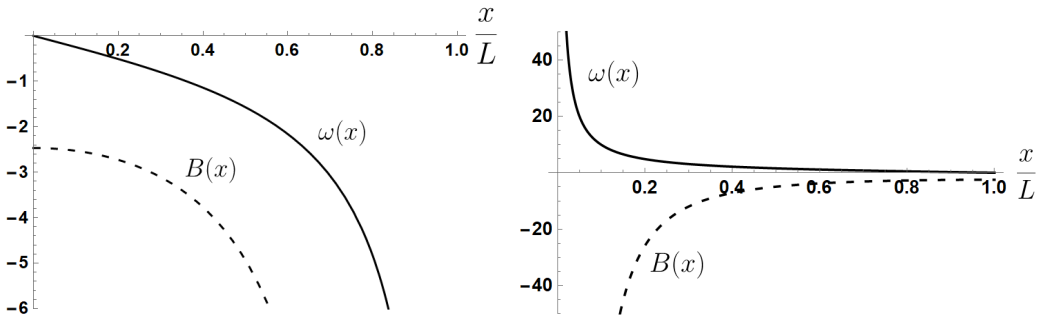


(a) $\alpha = \pi$ and $\sqrt{\xi - k_y^2} = \frac{1}{2}\pi$. (b) $\alpha = \frac{3}{2}\pi$ and $\sqrt{\xi - k_y^2} = \frac{1}{2}\pi$

**Figure 3.4.** Magnetic field $B_z(x)$ and function $\omega(x)$ for the studied examples.

of equation (3.1).

The expressions of the spinor components $\phi_n^{(A)}(x)$ and $\phi_n^{(B)}(x)$ are given by

$$\phi_n^{(A)}(x) = A\, \sin k_n\, x,$$

$$\phi_n^{(B)}(x) = -\frac{i\, A}{\bar{\epsilon}_n'^2}\left[k_n\, \cos k_n\, x - \sqrt{\xi - k_y^2}\cot\left(\sqrt{\xi - k_y^2}\, x\right)\, \sin k_n\, x\right].$$

In Figure 3.3 we show a plot of the modulus square of $\phi_n^{(A)}(x)$ and $\phi_n^{(B)}(x)$ for zero energy and for the first three lowest positive energies.

Finally, let us mention an interpretation of the effect of magnetic fields on charged particles has been given by Kuru, Nieto and Negro [36]. From classical electrodynamics, the Hamiltonian of a particle in a magnetic field is,

$$\mathbf{H} = \frac{1}{2}\left[\mathbf{p} - \mathbf{A}\right]^2 + V(\mathbf{r}).$$

The quantity,

$$\pi_y\,(x) = p_y - A_y(x),$$

is the kinetic momentum given by $m\,\dot{\mathbf{r}}$. The canonical momentum $p_y = k_y$ is a real constant and the vector potential $A_y(x) = \omega(x) - k_y$. Then,

$$\pi_y\,(x) = 2\,k_y - \omega(x).$$

As we can see in Figure 3.4, the function $\omega(x)$ is decreasing monotonic. If we consider $k_y = 0$ and a fixed point $x_0$ such that

$$\pi_y(x_0) = 0 \quad \rightarrow \quad \omega(x_0) = 0.$$

When $x \neq x_0$ the particle will move in the positive $y$ direction when $\omega(x)$ is negative and in the negative $y$ direction when $\omega(x)$ is positive and vice versa.

## 3.2 First + second SUSY transformation of a zigzag graphene nanoribbon

In Chapter 2 we introduced the supersymmetric quantum mechanics, a technique that intertwines two Schrödinger Hamiltonians. The intertwining procedure allows us to relate the eigenfunctions and eigenvalues of both Hamiltonians. So, if we know the eigenfunctions and eigenvalues of one of them we can obtain the corresponding ones of the other using the operators $L^{\pm}$. In this Section we will find the operator $L^{+}$, defined in equation (2.1), and we will make a first-order SUSY transformation to the Hamiltonian $\hat{H}_0^2$ of equation (3.1) to find its supersymmetric partner $\hat{H}_1^2$. We will apply $L^{+}$ to the solutions of $\hat{H}_0^2$, $\phi_n^{(A)}(x)$ from equation (3.2) or (3.3), to find the eigenfunctions of $\hat{H}_1^2$. Then we will do a second first-order SUSY transformation to find the Dirac Hamiltonian associated to $\hat{H}_1^2$, as we did for $\hat{H}_0^2$ in Section 3.1, and we will find the components of the spinor for this Dirac Hamiltonian.

We will work with a simplified version of the general expression of the solutions $\phi_n^{(A)}(x)$ of equation (3.1). The solution in the case of $z_n$ being a real number comes from equations (3.2),

$$\phi_n^{(A)}(x) = A \sinh z_n\, x + B \cosh z_n\, x.$$

The corresponding solution for the case when $z_n = i\, k_n$ being a pure imaginary number appears from equations (3.3),

$$\phi_n^{(A)}(x) = A \sin k_n\, x + B \cos k_n\, x.$$

The way to simplify $\phi_n^{(A)}(x)$ is to use only one constant for the initial conditions. Let us make the change of variable $A = \cosh\beta$ and $B = \sinh\beta$ for $z_n$ being a real number or $A = \cos\beta$ and $B = \sin\beta$ for $z_n = i\, k_n$. Therefore,

$$\phi_n^{(A)}(x) = \sinh\left(z_n\, x + \beta\right), \tag{3.23}$$

$$\phi_n^{(A)}(x) = \sin\left(k_n\, x + \beta\right). \tag{3.24}$$

The expression for the operator $L^+$ in equation (2.1) requires a superpotential $W(x)$, which is defined as

$$W(x) = \frac{u'^{(0)}\left(x\right)}{u^{(0)}\left(x\right)},$$

where the seed solution $u^{(0)}\left(x\right)$ fulfills the differential equation (3.1) without the constant $\xi$,

$$\left(-\frac{d^2}{dx^2} + k_y^2\right) u^{(0)}\left(x\right) = \bar{\epsilon}_\mu^2\, u^{(0)}\left(x\right).$$

When $z_\mu = \sqrt{k_y^2 - \bar{\epsilon}_\mu^2}$ is real the expression for the seed solution is,

$$u^{(0)}\left(x\right) = \cosh\left(z_\mu\, x + \gamma\right), \tag{3.25}$$

leading to the superpotential,

$$W(x) = z_\mu \tanh\left(z_\mu\, x + \gamma\right). \tag{3.26}$$

However, if $z_\mu = i\, k_\mu$ is a pure imaginary number it turns out that

$$u^{(0)}\left(x\right) = \cos\left(k_\mu\, x + \gamma\right), \tag{3.27}$$

and the superpotential becomes

$$W(x) = -k_\mu \tan\left(k_\mu\, x + \gamma\right). \tag{3.28}$$

The expressions of these superpotentials are similar to those of $\omega(x)$ that we saw in equations (3.7) and (3.10). The reason is that the seed solutions that define them solve the same differential equation. The difference is that $\omega(x)$ was used to find the Dirac Hamiltonian of $\hat{H}_0^2$ and the $W(x)$ we are using allows to know the operators $L^\pm$ and find the supersymmetric partners of $\hat{H}_0^2$.

The interwining operators $L^\pm$ are defined as,

$$L^+ = -\frac{d}{dx} + W(x), \qquad L^- = \frac{d}{dx} + W(x),$$

and the factorization relationships between the intertwined Hamiltonians and the operators $L^\pm$ are

$$\hat{H}_0^2 - \bar{\epsilon}_\mu^2 = L^-\, L^+, \qquad \hat{H}_1^2 - \bar{\epsilon}_\mu^2 = L^+\, L^-.$$

We can find now the relationship between the potentials of the Schrödinger Hamiltonians and $\omega(x)$ because,

$$L^- L^+ = -\frac{d^2}{dx^2} + W'(x) + W^2(x), \qquad L^+ L^- = -\frac{d^2}{dx^2} - W'(x) + W^2(x).$$

Therefore, from relations (2.4) we have,

$$V_1(x) = V_0(x) - 2\,W'(x).$$

If we replace the potential $V_0(x) = k_y'^2$ from equation (3.1) and the derivative of the function $W(x)$ of equation (3.26) it is obtained

$$V_1(x) = k_y^2 - \xi - 2\,z_\mu^2\,\mathrm{sech}^2\left(z_\mu\,x + \gamma\right),$$

when $z_\mu$ is real. The Schrödinger equation for $\hat{H}_1^2$ takes the form

$$\hat{H}_1^2\,\phi_n^{(A,1)}(x) = \left[-\frac{d^2}{dx^2} + k_y'^2 - 2\,z_\mu^2\,\mathrm{sech}^2\left(z_\mu\,x + \gamma\right)\right]\phi_n^{(A,1)}(x) = \bar{\epsilon}_n'^2\,\phi_n^{(A,1)}(x). \tag{3.29}$$

When $z_\mu = i\,k_\mu$ being a pure imaginary number,

$$V_1(x) = k_y^2 - \xi + 2\,k_\mu^2\,\sec^2\left(k_\mu\,x + \gamma\right),$$

$$\hat{H}_1^2\,\phi_n^{(A,1)}(x) = \left[-\frac{d^2}{dx^2} + k_y'^2 + 2\,k_\mu^2\,\sec^2\left(k_\mu\,x + \gamma\right)\right]\phi_n^{(A,1)}(x) = \bar{\epsilon}_n'^2\,\phi_n^{(A,1)}(x), \tag{3.30}$$

where $\bar{\epsilon}_n'^2 = k_y'^2 - z_n^2$. The potentials that we have obtained in equation (3.29) are known as hyperbolic Pöschl-Teller potentials while are called trigonometric Pöschl-Teller potentials those of equation (3.30) [38, 39, 40]. Our $x$-interval is limited to the width $L$ of the nanoribbons, so the potentials are truncated.

Now we will apply a second first-order SUSY transformation to obtain the Dirac Hamiltonian $\hat{H}_D^{(1)}$ of $\hat{H}_1^2$ and the spinor components that satisfy the boundary conditions (1.5) plus its energy spectrum. We will take the solutions of the Schrödinger equation (3.29) or (3.30), which are given by

$$\phi_n^{(A,1)}(x) = \frac{L^+\,\phi_n^{(A)}(x)}{\sqrt{\bar{\epsilon}_n^2 - \bar{\epsilon}_\mu^2}},$$

as the upper spinor component of the Dirac Hamiltonian $\hat{H}_D^{(1)}$. The solution $\phi_n^{(A,1)}(x)$ has four possible expressions:

- When $z_n$ and $z_\mu$ are real numbers we have

$$\begin{aligned}\phi_n^{(A,1)}(x) = \; & \tfrac{1}{\sqrt{\bar{\epsilon}_n^2-\bar{\epsilon}_\mu^2}}\left[-z_n\,\cosh\left(z_n\,x+\beta\right)\right. \\ & \left.+z_\mu\,\tanh\left(z_\mu\,x+\gamma\right)\sinh\left(z_n\,x+\beta\right)\right].\end{aligned} \tag{3.31}$$

- If $z_n$ is a real number and $z_\mu = i\,k_\mu$ is a pure imaginary number we obtain

$$\begin{aligned}\phi_n^{(A,1)}(x) = \; & \tfrac{1}{\sqrt{\bar{\epsilon}_n^2-\bar{\epsilon}_\mu^2}}\left[-z_n\cosh\left(z_n\,x+\beta\right)\right. \\ & \left.-k_\mu\tan\left(k_\mu\,x+\gamma\right)\sinh\left(z_n\,x+\beta\right)\right].\end{aligned} \tag{3.32}$$

- In the case that $z_n = i\,k_n$ is a pure imaginary number and $z_\mu$ is a real number we arrive at

$$\begin{aligned}\phi_n^{(A,1)}(x) = \; & \tfrac{1}{\sqrt{\bar{\epsilon}_n^2-\bar{\epsilon}_\mu^2}}\left[-k_n\cos\left(k_n\,x+\beta\right)\right. \\ & \left.+z_\mu\tanh\left(z_\mu\,x+\gamma\right)\,\sin\left(k_n\,x+\beta\right)\right].\end{aligned} \tag{3.33}$$

- Finally, if both $z_n = i\,k_n$ and $z_\mu = i\,k_\mu$ are pure imaginary numbers we end up with

$$\begin{aligned}\phi_n^{(A,1)}(x) = \; & \tfrac{1}{\sqrt{\bar{\epsilon}_n^2-\bar{\epsilon}_\mu^2}}\left[-k_n\,\cos\left(k_n\,x+\beta\right)\right. \\ & \left.-k_\mu\,\tan\left(k_\mu\,x+\gamma\right)\,\sin\left(k_n\,x+\beta\right)\right].\end{aligned} \tag{3.34}$$

The lower entry of the spinor is obtained from equation (1.27) and a function $\omega_1(x)$ such that:

$$\omega_1(x) = \frac{\nu_1'(x)}{\nu_1(x)}, \tag{3.35}$$

where $\nu_1(x)$ is the solution to the differential equation,

$$\left(-\frac{d^2}{dx^2}+V_1(x)\right)\nu_1(x) = 0. \tag{3.36}$$

If $z_\mu$ is a real number such differential equation is given by,

$$\left[-\frac{d^2}{dx^2}+k_y^2-2\,z_\mu^2\,\mathrm{sech}^2\left(z_\mu\,x+\gamma\right)\right]\nu_1(x) = \xi\,\nu_1(x). \tag{3.37}$$

In the case that $z_\mu = i\,k_\mu$ is a pure imaginary number we arrive at

$$\left[-\frac{d^2}{dx^2} + k_y^2 + 2\,k_\mu^2\,\sec^2\left(k_\mu\,x+\gamma\right)\right]\nu_1(x) = \xi\,\nu_1(x). \tag{3.38}$$

Note that these equations are similar to equations (3.29) and (3.30) but with energy $\bar{\epsilon}_n^2 = \xi$. Therefore, the function $\nu_1(x)$ is any solution appearing in equations (3.31) to (3.34) with the change $z_n = \sqrt{k_y^2 - \bar{\epsilon}_n} \to \sqrt{k_y^2 - \xi}$. The following is a list with the different possible cases.

- If $\sqrt{k_y^2-\xi}$ and $z_\mu$ are real numbers we will have:

$$\begin{aligned}\nu_1\left(x\right) = \; & -\sqrt{k_y^2-\xi}\,\cosh\left(\sqrt{k_y^2-\xi}\,x+\delta\right) \\ & +z_\mu\,\tanh\left(z_\mu\,x+\gamma\right)\sinh\left(\sqrt{k_y^2-\xi}\,x+\delta\right).\end{aligned} \tag{3.39}$$

- In case that $\sqrt{k_y^2-\xi}$ is a real number and $z_\mu = i\,k_\mu$ it is obtained:

$$\begin{aligned}\nu_1\left(x\right) = \; & -\sqrt{k_y^2-\xi}\,\cosh\left(\sqrt{k_y^2-\xi}\,x+\delta\right) \\ & -k_\mu\tan\left(k_\mu\,x+\gamma\right)\sinh\left(\sqrt{k_y^2-\xi}\,x+\delta\right).\end{aligned} \tag{3.40}$$

- When $\sqrt{k_y^2-\xi}$ is an imaginary number and $z_\mu$ a real number we arrive at:

$$\begin{aligned}\nu_1\left(x\right) = \; & -\sqrt{\xi-k_y^2}\,\cos\left(\sqrt{\xi-k_y^2}\,x+\delta\right) \\ & +z_\mu\tanh\left(z_\mu\,x+\gamma\right)\,\sin\left(\sqrt{\xi-k_y^2}\,x+\delta\right).\end{aligned} \tag{3.41}$$

- For $\sqrt{k_y^2-\xi}$ being an imaginary number and $z_\mu = i\,k_\mu$ it turns out that:

$$\begin{aligned}\nu_1\left(x\right) = \; & -\sqrt{\xi-k_y^2}\,\cos\left(\sqrt{\xi-k_y^2}\,x+\delta\right) \\ & -k_\mu\,\tan\left(k_\mu\,x+\gamma\right)\,\sin\left(\sqrt{\xi-k_y^2}\,x+\delta\right).\end{aligned} \tag{3.42}$$

The lower component of the spinor of $\hat{H}_D^{(1)}$ is obtained from equation (1.27):

$$\phi_n^{(B,1)}(x) = -\frac{i}{\sqrt{\hat{\epsilon}_n^2-\xi}}\left(\frac{d\,\phi_n^{(A,1)}(x)}{dx} - \omega_1(x)\;\phi_n^{(A,1)}(x)\right).$$

In the same way as for $\phi_n^{(A,1)}(x)$, we have four possible cases for $\phi_n^{(B,1)}(x)$.

- When $z_n$ and $z_\mu$ are real numbers it is obtained:

$$\begin{aligned}\phi_n^{(B,1)}(x) = & \frac{i\,\sinh(z_n\,x+\beta)}{\sqrt{(\bar{\epsilon}_n^2-\xi)\left(\bar{\epsilon}_n^2-\bar{\epsilon}_\mu^2\right)}}\left[z_n^2 - z_\mu^2\,\mathrm{sech}^2\,\left(\,z_\mu\,x+\gamma\,\right)\right. \\ & \left.+\,\omega_1\left(x\right)z_\mu\tanh\,\left(z_\mu x+\gamma\right)\right] - \frac{i\,\cosh\left(z_n\,x+\beta\right)}{\sqrt{(\bar{\epsilon}_n^2-\xi)\left(\bar{\epsilon}_n^2-\bar{\epsilon}_\mu^2\right)}} \\ & \times\left[z_n\,z_\mu\tanh\,\left(z_\mu\,x+\gamma\right)+z_n\,\omega_1\left(x\right)\right].\end{aligned} \tag{3.43}$$

- In the case that $z_n$ is a real number and $z_\mu = i\,k_\mu$ a pure imaginary number we obtain:

$$\begin{aligned}\phi_n^{(B,1)}(x) = & \frac{i\,\sinh(z_n\,x+\beta)}{\sqrt{(\bar{\epsilon}_n^2-\xi)\left(\bar{\epsilon}_n^2-\bar{\epsilon}_\mu^2\right)}}\left[z_n^2 + k_\mu^2\,\mathrm{sec}^2\,\left(\,k_\mu\,x+\gamma\,\right)\right. \\ & \left.-\,\omega_1\left(x\right)k_\mu\tan\,\left(k_\mu x+\gamma\right)\right] + \frac{i\,\cosh\left(z_n\,x+\beta\right)}{\sqrt{(\bar{\epsilon}_n^2-\xi)\left(\bar{\epsilon}_n^2-\bar{\epsilon}_\mu^2\right)}} \\ & \times\left[z_n\,k_\mu\tan\,\left(k_\mu\,x+\gamma\right)-\,z_n\,\omega_1\left(x\right)\right].\end{aligned} \tag{3.44}$$

- For $z_n = i\,k_n$ being a pure imaginary number and $z_\mu$ a real number we arrive at:

$$\begin{aligned}\phi_n^{(B,1)}(x) = & \frac{i\,\sin(k_n\,x+\beta)}{\sqrt{(\bar{\epsilon}_n^2-\xi)\left(\bar{\epsilon}_n^2-\bar{\epsilon}_\mu^2\right)}}\left[-k_n^2 - z_\mu^2\,\mathrm{sech}^2\,\left(\,z_\mu\,x+\gamma\,\right)\right. \\ & \left.+\,\omega_1\left(x\right)z_\mu\tanh\,\left(z_\mu x+\gamma\right)\right] - \frac{i\,\cos\left(k_n\,x+\beta\right)}{\sqrt{(\bar{\epsilon}_n^2-\xi)\left(\bar{\epsilon}_n^2-\bar{\epsilon}_\mu^2\right)}} \\ & \times\left[k_n\,z_\mu\tanh\,\left(z_\mu\,x+\gamma\right)+\,k_n\,\omega_1\left(x\right)\right].\end{aligned} \tag{3.45}$$

- If both $z_n = i\,k_n$ and $z_\mu = i\,k_\mu$ are pure imaginary numbers we will have:

$$\begin{aligned}\phi_n^{(B,1)}(x) = & \frac{i\,\sin(k_n\,x+\beta)}{\sqrt{(\bar{\epsilon}_n^2-\xi)\left(\bar{\epsilon}_n^2-\bar{\epsilon}_\mu^2\right)}}\left[-k_n^2 + k_\mu^2\,\mathrm{sec}^2\,\left(\,k_\mu\,x+\gamma\,\right)\right. \\ & \left.-\,\omega_1\left(x\right)k_\mu\tan\,\left(k_\mu x+\gamma\right)\right] + \frac{i\,\cos\left(k_n\,x+\beta\right)}{\sqrt{(\bar{\epsilon}_n^2-\xi)\left(\bar{\epsilon}_n^2-\bar{\epsilon}_\mu^2\right)}} \\ & \times\left[k_n\,k_\mu\tan\,\left(k_\mu\,x+\gamma\right)-\,k_n\,\omega_1\left(x\right)\right].\end{aligned} \tag{3.46}$$

### 3.2.1 The zeros of $\nu_1\left(x\right)$

Two seed solutions have been used in this section, the functions $u^{(0)}\left(x\right)$ and $\nu_1(x)$. To generate a well behaved Dirac Hamiltonian $\hat{H}_D^{(1)}$ both seed solutions must be nodeless in $x \in [0,1]$, otherwise the auxiliary potential $V_1(x)$ and the

vector potential $A_y(x) = \omega(x) - k_y$ will be singular at the node positions, see equations (3.35) and (3.36).

The conditions on the allowed functions $u^{(0)}(x)$ of equations (3.25) and (3.27) are shown in Table 3.1. The seed solutions $\nu_1(x)$ of equations (3.39) to (3.42) have values of $x$ where they vanish. We can identify them if we solve the following equations:

- For the case of equation (3.39) we have

$$\sqrt{k_y^2 - \xi}\, \coth\left(\sqrt{k_y^2 - \xi}\, x + \delta\right) = z_\mu\, \tanh\left(z_\mu\, x + \gamma\right). \tag{3.47}$$

- If the equation is (3.40) it turns out that:

$$\sqrt{k_y^2 - \xi}\, \coth\left(\sqrt{k_y^2 - \xi}\, x + \delta\right) = k_\mu\, \cot\left(k_\mu\, x + \gamma + \frac{\pi}{2}\right). \tag{3.48}$$

- For equation (3.41) it should be fulfilled:

$$\sqrt{\xi - k_y^2}\, \cot\left(\sqrt{\xi - k_y^2}\, x + \delta\right) = z_\mu\, \tanh\left(z_\mu\, x + \gamma\right). \tag{3.49}$$

- In case of equation (3.42) we must have:

$$\sqrt{\xi - k_y^2}\, \cot\left(\sqrt{\xi - k_y^2}\, x + \delta\right) = k_\mu\, \cot\left(k_\mu\, x + \gamma + \frac{\pi}{2}\right). \tag{3.50}$$

If a point $x_p$ satisfies one of the equations shown above, then $\nu_1(x_p) = 0$ and $\omega_1(x_p) = \nu_1'(x_p)/\nu_1(x_p) \to \infty$. We were not able to find a general condition on the parameters $\gamma$, $\delta$, $\xi$ and $z_\mu$, but some cases can be completely studied. One simple example is when $\delta = \gamma + \pi/2$ and $k_\mu = \sqrt{\xi - k_y^2}$ for (3.50).

Although it is better to study equations (3.48) to (3.50) numerically, the condition (3.47) can be as well fully analyzed. In order that $\nu_1(x)$ in equation (3.39) is not zero at some point in $(0, 1)$, we need that $I = \sqrt{k_y^2 - \xi}/z_\mu > 1$. If $I$ is less than 1 and positive then $\delta \leq -\sqrt{k_y^2 - \xi}$ and $\gamma \geq 0$ are sufficient to ensure that $\nu_1(x) \neq 0$ for all $x$ in $[0, 1]$. The reason is because the hyperbolic cotangent function has its divergence at $x_\delta = -\delta/\sqrt{k_y^2 - \xi}$. When $\delta$ is less than $-\sqrt{k_y^2 - \xi}$, the positive part of the hyperbolic cotangent function is

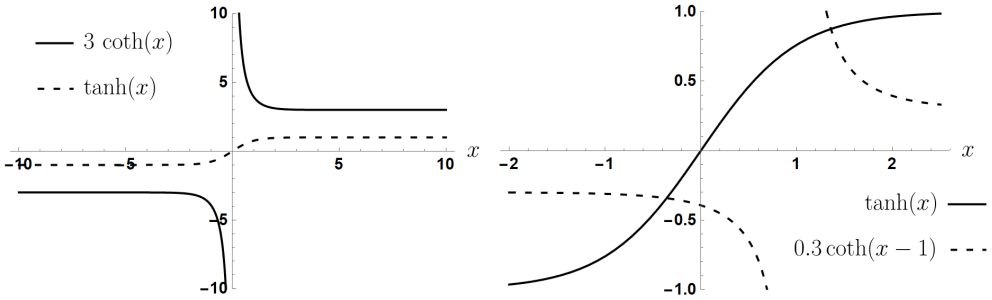


(a) $\sqrt{k_y^2 - \xi}$, $z_\mu$ real numbers and $I = 3$. (b) $\sqrt{k_y^2 - \xi}$, $z_\mu$ real numbers and $I = 0.3$.

**Figure 3.5.** Plot of cases where the functions $I \coth(x + \delta)$ and $\tanh(x + \gamma)$ intersect to each other. In both examples it has been taken $\gamma = 0$ for convenience. In the points $x_p$ where they intersect the function $\nu_1(x)$ becomes zero.

outside the interval $[0, 1]$. Thus, the negative part does not intercept with the hyperbolic tangent function if $\gamma \geq 1$ because the point where the hyperbolic tangent is zero is shifted to the left of the interval $[0, 1]$. Two examples can be seen in Figure 3.5, one with $I > 1$ and the other with $I < 1$.

### 3.2.2 Zigzag boundary conditions

The boundary conditions $\phi_n^{(A,1)}(0) = 0$ and $\phi_n^{(B,1)}(1) = 0$ of equation (1.5) for the components of the spinor $\Phi(x)$ of equation (1.8) give us a transcendental equation for each component. The following list represents the transcendental equation coming from $\phi_n^{(A,1)}(0) = 0$.

- If we have that $z_n$ and $z_\mu$ are real numbers then,

$$z_n \coth \beta = z_\mu \tanh \gamma. \tag{3.51}$$

- In the case where $z_n$ is a real number and $z_\mu = i\, k_\mu$ is a pure imaginary number it turns out that:

$$z_n \coth \beta = k_\mu \cot\left(\gamma + \frac{\pi}{2}\right). \tag{3.52}$$

- When $z_n = i\, k_n$ is a pure imaginary number and $z_\mu$ is a real number we have:

$$k_n \cot \beta = z_\mu \tanh \gamma. \tag{3.53}$$

- If $z_n$ and $z_\mu$ are pure imaginary numbers it must be fulfilled that

$$k_n \cot \beta = k_\mu \cot \left(\gamma + \frac{\pi}{2}\right). \tag{3.54}$$

There is not a general expression telling us what values of $z_n$, $z_\mu$, $\beta$ and $\gamma$ solve these equations. However, some particular values of the parameters $\beta$ and $\gamma$ simplify such equations. One case is when $\beta = 0$. In this case the hyperbolic cotangent function of equation (3.51) diverges while the hyperbolic tangent function is bounded, then (3.51) cannot be satisfied. In the same way, equation (3.53) cannot be fulfilled because the cotangent function diverges. Instead, equations (3.52) and (3.54) are satisfied when $\beta = 0$ and $\gamma = (m + 1/2)\,\pi$ with $m$ being an integer, since then the right hand side of both equations becomes $\cot[(m+1)\pi]$.

A second case where we can simplify equations (3.51) to (3.54) is taking the parameters $\beta = \pi/2$ and $\gamma = 0$. If $\gamma = 0$ the hyperbolic tangent function of equations (3.51) and (3.53) becomes zero, but for $\beta = \pi/2$ the hyperbolic cotangent function is different from zero and thus (3.51) cannot be satisfied. However equation (3.53) is fulfilled because $\cot \pi/2 = 0$. This also happens for equations (3.52) and (3.54). Equation (3.52) cannot be satisfied because $\cot \pi/2 = 0$ and $\coth \pi/2 \neq 0$, while equation (3.54) is fulfilled.

The boundary condition $\phi_n^{(B,1)}(1) = 0$ for the lower spinor component gives us the following transcendental equations:

- In the case where $z_n$ and $z_\mu$ are real numbers the transcendental equation is,

$$\coth\,(z_n + \beta) = \frac{z_n^2 - z_\mu^2\,\operatorname{sech}^2\,(z_\mu + \gamma) + z_\mu\,\omega_1\,(1)\tanh\,(z_\mu + \gamma)}{z_n\,\omega_1\,(1) + z_n\,z_\mu\,\tanh\,(z_\mu + \gamma)}. \tag{3.55}$$

- Instead, if $z_n$ is a real number and $z_\mu = i\,k_\mu$ is a pure imaginary number we obtain:

$$\coth\,(z_n + \beta) = \frac{z_n^2 + k_\mu^2\,\sec^2\,(k_\mu + \gamma) - k_\mu\,\omega_1\,(1)\tan\,(k_\mu + \gamma)}{z_n\,\omega_1\,(1) - z_n\,k_\mu\,\tan\,(k_\mu + \gamma)}. \tag{3.56}$$

- For $z_n = i\,k_n$ being is a pure imaginary number and $z_\mu$ a real number the transcendental equation to be solved is:

$$\cot\,(k_n+\beta) = \frac{-k_n^2 - z_\mu^2\,\operatorname{sech}^2\,(z_\mu+\gamma) + z_\mu\,\omega_1\,(1)\tanh\,(z_\mu+\gamma)}{k_n\,\omega_1\,(1) + k_n\,z_\mu\,\tanh\,(z_\mu+\gamma)}. \tag{3.57}$$

- The last situation is when $z_n$ and $z_\mu$ are pure imaginary numbers for which:

$$\cot\,(k_n+\beta) = \frac{-k_n^2 + k_\mu^2\,\sec^2\,(k_\mu+\gamma) - k_\mu\,\omega_1\,(1)\tan\,(k_\mu+\gamma)}{k_n\,\omega_1\,(1) - k_n\,k_\mu\,\tan\,(k_\mu+\gamma)}. \tag{3.58}$$

For each case, we must solve the corresponding equation for $z_n$, assuming that we know the values of the parameters $z_\mu$, $\beta$ and $\gamma$. There is no single way to solve these transcendental equations because, they are as well related with equations (3.47) to (3.50) and equations (3.51) to (3.54).

### 3.2.3 Examples

Let us see a simple example, for the phases $\beta = \delta = \pi/2$ and $\gamma = 0$. This choice simplifies and solves the transcendental equations (3.53) and (3.54), associated to the condition $\phi_n^{(A,1)}(0) = 0$, and allows us to choose $z_\mu$ and $z_n = i\,k_n$ independently. Note that we can use $z_\mu$ as a real or pure imaginary number, but $z_n$ is always pure imaginary.

Equations (3.47) to (3.50), about the zeros of the seed solution $\nu_1(x)$, limit the values of $z_\mu$.

- If $\sqrt{k_y^2-\xi}$ and $z_\mu$ are real numbers then:

$$-\sqrt{k_y^2-\xi} < z_\mu < \sqrt{k_y^2-\xi}.$$

- When $\sqrt{k_y^2-\xi}$ is a real number and $z_\mu = i\,k_\mu$ it turns out that:

$$-\frac{\pi}{2} \leq k_\mu \leq \frac{\pi}{2}, \qquad \sqrt{k_y^2-\xi} \in \mathbb{R}\setminus(-|k_\mu|,0), \qquad \sqrt{k_y^2-\xi} \neq k_\mu.$$

- In the case that $\sqrt{\xi-k_y^2}$ and $z_\mu$ are both real numbers it is obtained:

$$z_\mu \in \mathbb{R}, \qquad -\frac{\pi}{2} \leq \sqrt{\xi-k_y^2} \leq \frac{\pi}{2}.$$

- Instead, if $\sqrt{\xi - k_y^2}$ is a real number and $z_\mu = i\,k_\mu$ we arrive at:

$$\sqrt{\xi - k_y^2} \in [-\pi, \pi], \qquad k_\mu \in [-\pi, \pi], \qquad \sqrt{\xi - k_y^2} \neq k_\mu.$$

As we can see, we have available many options, but for simplicity we will choose the last case with $k_\mu = 4\pi/10$ and $\sqrt{\xi - k_y^2} = 3\pi/10$. The seed solution $\nu_1(x)$ will be,

$$\nu_1\left(x\right) = a\,\sin\,ax - b\,\tan\,b\,x\,\cos\,ax, \qquad a = \frac{3}{10}\,\pi, \qquad b = \frac{4}{10}\pi.$$

The superpotential $\omega_1\left(x\right) = \nu_1'(x)/\nu_1(x)$ becomes:

$$\omega_1\left(x\right) = \frac{a^2\,\cos\,ax + a\,b\,\tan\,b\,x\,\sin\,ax - b^2\,\sec^2\,bx\,\cos\,ax}{a\,\sin\,ax - b\,\tan\,b\,x\,\cos\,a\,x}.$$

Now, equation (3.46) supplies us the expression for the lower spinor component $\phi_n^{(B,1)}(x)$, while the Dirac Hamiltonian is given by equation (1.20),

$$\hat{H}_D^{(1)} = -i\sigma_x\frac{d}{dx} + \sigma_y\,\omega(x).$$

The transcendental equation (3.58) associated to the condition $\phi_n^{(B,1)}(1) = 0$, can be solved straight forwardly. We can write it as follows

$$\cot\left(k_n + \frac{\pi}{2}\right) = \kappa\left(k_n\right),$$

where,

$$\kappa\left(k_n\right) = \frac{-k_n^2 + k_\mu^2\,\sec^2\,\left(k_\mu\right) - k_\mu\,\omega_1\left(1\right)\tan\,\left(k_\mu\right)}{k_n\,\omega_1\left(1\right) - k_n\,k_\mu\,\tan\,\left(k_\mu\right)}.$$

This equation is solved numerically for $k_n$, generating the following list of solutions

$$k_n = \{\pm\,0.9425,\,\pm\,4.6532,\,\pm\,7.8193,\,\pm\,10.9710,\,\cdots\},$$

where $n = \pm 1, \pm 2, \cdots$. In Figure 3.6 (a) we can see the first solutions of such transcendental equation.

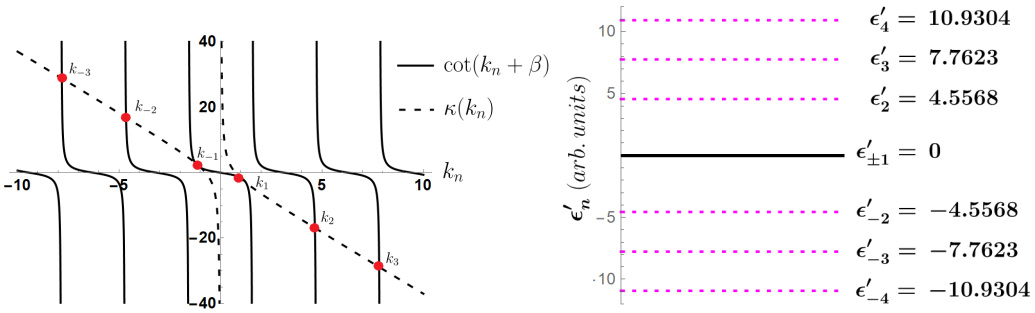


(a) $z_n = i\,k_n$. (b) Energy spectrum.

**Figure 3.6.** (a) Solutions of the transcendental equation obtained from the condition $\phi_n^{(B,1)}(1) = 0$ for $z_n = i\,k_n$ and (b) energy spectrum. We use the parameters $\beta = \delta = \frac{1}{2}\,\pi$, $\gamma = 0$, $k_\mu = \frac{4}{10}\,\pi$ and $\sqrt{\xi - k_y^2} = \frac{3}{10}\pi$.

The energy spectrum for the Dirac Hamiltonian is given by $\epsilon'_n = \pm\sqrt{k_y^2 + k_n^2 - \xi}$. We do not know the value of $k_y$ or the value of $\xi$ separately, what we know is the value of $\sqrt{\xi - k_y^2} = 3\pi/10$. Thus, the energy expression is given by

$$\epsilon'_n = \sqrt{k_n^2 - (\xi - k_y^2)} = \sqrt{k_n^2 - \frac{9}{100}\pi^2}$$

We are also in position to know the spinor components, which are given by equations (3.34) and (3.46). Their explicit form are:

$$\phi_n^{(A,1)}(x) = \frac{1}{\sqrt{\bar{\epsilon}'^{\,2}_n - \bar{\epsilon}'^{\,2}_\mu}}\left[k_n \sin k_n\, x - k_\mu \tan k_\mu\, x \cos k_n\, x\right],$$

$$\begin{aligned}\phi_n^{(B,1)}(x) = \; & \frac{i\cos k_n\, x}{\sqrt{(\bar{\epsilon}_n^2 - \xi)\left(\bar{\epsilon}'^{\,2}_n - \bar{\epsilon}'^{\,2}_\mu\right)}}\left[-k_n^2 + k_\mu^2 \sec^2 k_\mu\, x - \omega_1(x)\, k_\mu \tan k_\mu x\right] \\ & - \frac{i\sin k_n\, x}{\sqrt{(\bar{\epsilon}_n^2 - \xi)\left(\bar{\epsilon}'^{\,2}_n - \bar{\epsilon}'^{\,2}_\mu\right)}}\left[k_n\, k_\mu \tan k_\mu\, x - k_n\, \omega_1(x)\right].\end{aligned}$$

We take the energy parameter $\bar{\epsilon}'_\mu = \sqrt{k_\mu^2 - (\xi - k_y^2)} = 0.8312$. The energy levels $\bar{\epsilon}'_{\pm 1} = \pm\sqrt{\bar{\epsilon}_{\pm 1}^2 - \xi}$ for $k_{\pm 1} = \pm 0.9425$ are zero. Therefore, the 1-SUSY transformation to obtain the Schrödinger Hamiltonian $\hat{H}_1^2$ deletes the ground state $\bar{\epsilon}_1^2$ of the Schrödinger Hamiltonian $\hat{H}_0^2$ because $k_1 = \sqrt{\xi - k_y^2}$. This means that the spinor component $\phi_n^{(B,1)}(x)$ is not defined for $n = \pm 1$. In

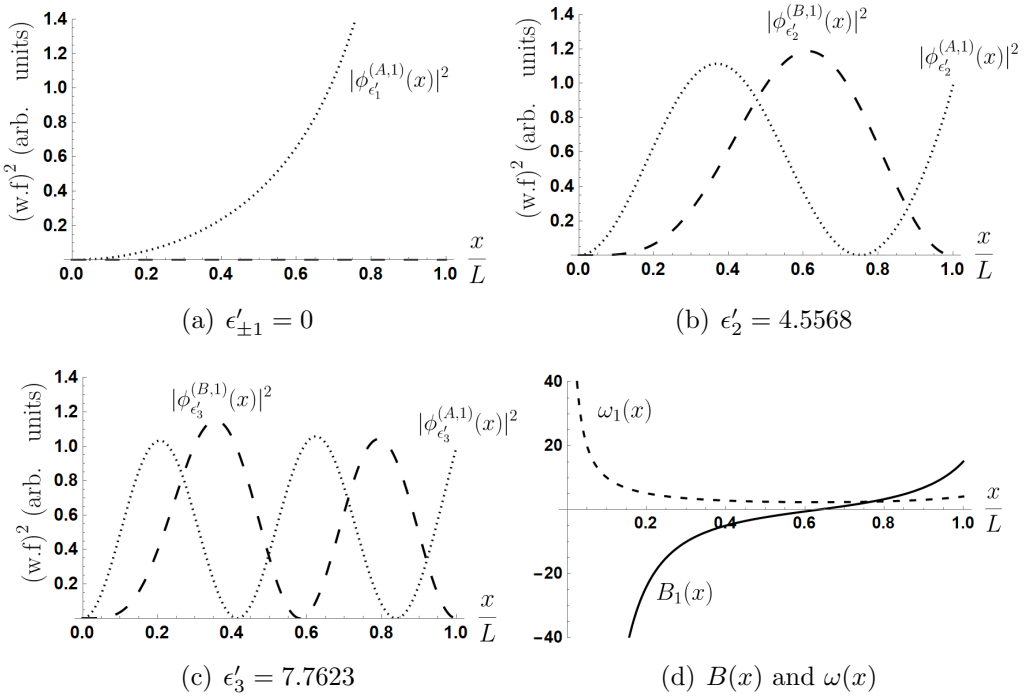


(a) $\epsilon'_{\pm 1} = 0$ (b) $\epsilon'_2 = 4.5568$

(c) $\epsilon'_3 = 7.7623$ (d) $B(x)$ and $\omega(x)$

**Figure 3.7.** (a)-(c) Modulus square of the normalized spinor components $\phi_n^{(A,1)}(x)$ and $\phi_n^{(B,1)}(x)$. (d) Magnetic field $B_1(x)$ and superpotential $\omega_1(x)$ of the SUSY transformation. The parameters are taken as $\beta = \frac{1}{2}\pi$, $\gamma = 0$, $\delta = \frac{1}{2}\pi$, $k_\mu = \frac{4}{10}\pi$ and $\sqrt{\xi - k_y^2} = \frac{3}{10}\pi$.

Figure 3.7 (a) to (c) we can see the modulus square of the spinor components $\phi_n^{(A,1)}(x)$ and $\phi_n^{(B,1)}(x)$ for the first three positive values of $n$.

About the magnetic field, in equation (3.12) we saw that the derivative of the function $\omega_1(x)$ gives us the magnetic field expression:

$$\mathbf{B}_1(x) = \frac{d\,\omega_1(x)}{dx}\,\hat{e}_z.$$

In Figure 3.7 (d) we can see a plot of both, the magnetic field $B_1(x)$ and $\omega_1(x)$. The graph shows that $\omega_1(x)$ approaches infinity at $x = 0$, which means that $\nu_1(x)$ has a zero at $x = 0$.

In the second example we select values of $\beta$ and $\gamma$ inside the allowed intervals but without any peculiarity that simplifies equations (3.51) to (3.54). One way to work is to solve for $z_\mu$ in the equations, leading to four different cases

- In the case where $z_n$ and $z_\mu$ are real numbers it is obtained:

$$z_\mu = z_n \coth\,\beta\,\coth\,\gamma. \tag{3.59}$$

- When $z_n$ is a real number and $z_\mu = i\,k_\mu$ is a pure imaginary number we arrive at:

$$k_\mu = z_n \coth\,\beta\,\tan\,(\gamma + \frac{\pi}{2}). \tag{3.60}$$

- If $z_n = i\,k_n$ is a pure imaginary number and $z_\mu$ is a real number it turns out that:

$$z_\mu = k_n\,\cot\,\beta\,\coth\,\gamma. \tag{3.61}$$

- Instead, if $z_n$ and $z_\mu$ are pure imaginary numbers we get:

$$k_\mu = k_n\,\cot\,\beta\tan\,(\gamma + \frac{\pi}{2}). \tag{3.62}$$

This approach is not the most suitable, since we want our parameters to affect only the entries of the spinor and the energy spectrum of the Dirac Hamiltonian. The parameter $z_\mu$ appears in the expressions for the superpotential $W(x)$, equations (3.26) and (3.28), in the supersymmetric partner $\hat{H}_1^2$, equations (3.29) and (3.30), in the spinor components $\phi_n^{(A,1)}(x)$ and $\phi_n^{(B,1)}(x)$,

equations (3.31) to (3.34) and (3.43) to (3.46), and in the function $\omega_1(x)$. Therefore, each value of $z_n$ gives us a different value of $z_\mu$ and thus a solution for a different Dirac Hamiltonian.

A better option is to solve equations (3.51) to (3.54) for $\beta$.

- When $z_n$ and $z_\mu$ are real numbers we obtain:

$$\beta(z_n) = \operatorname{arcoth}\left(\frac{z_\mu}{z_n}\tanh\,\gamma\right). \tag{3.63}$$

- If $z_n$ is a real number and $z_\mu = i\,k_\mu$ is a pure imaginary number we arrive at:

$$\beta(z_n) = \operatorname{arcoth}\left(\frac{k_\mu}{z_n}\cot\,(\gamma+\frac{\pi}{2})\right). \tag{3.64}$$

- In the case where $z_n = i\,k_n$ is a pure imaginary number and $z_\mu$ is a real number it turns out that:

$$\beta(k_n) = \operatorname{arccot}\left(\frac{z_\mu}{k_n}\,\tanh\,\gamma\right). \tag{3.65}$$

- Instead, if $z_n$ and $z_\mu$ are pure imaginary numbers we get:

$$\beta(k_n) = \operatorname{arccot}\left(\frac{k_\mu}{k_n}\cot\,(\gamma+\frac{\pi}{2})\right). \tag{3.66}$$

In these equations we select constant values for $\gamma$ and $z_\mu$ leaving $\beta$ as function of $z_n$. Since the parameter $\beta(z_n)$ only affects the entries of the spinor, it is our best option.

To illustrate the procedure, let us fix the parameters $\gamma = \frac{2}{5}\pi$, $\delta = -\frac{2}{5}\pi$, $k_\mu = -\frac{3}{5}\pi$ and $\sqrt{k_y^2-\xi} = \frac{7}{10}\pi$. As $z_\mu$ is a pure imaginary number and $k_y^2-\xi > 0$, it turns out that:

$$\begin{aligned} W(x) = &\ -k_\mu\tan\left(k_\mu\,x+\gamma\right), \\ \nu_1\,(x) = &\ -\sqrt{k_y^2-\xi}\,\cosh\left(\sqrt{k_y^2-\xi}\,x+\delta\right) \\ &\ -k_\mu\tan\left(k_\mu\,x+\gamma\right)\sinh\left(\sqrt{k_y^2-\xi}\,x+\delta\right). \end{aligned}$$

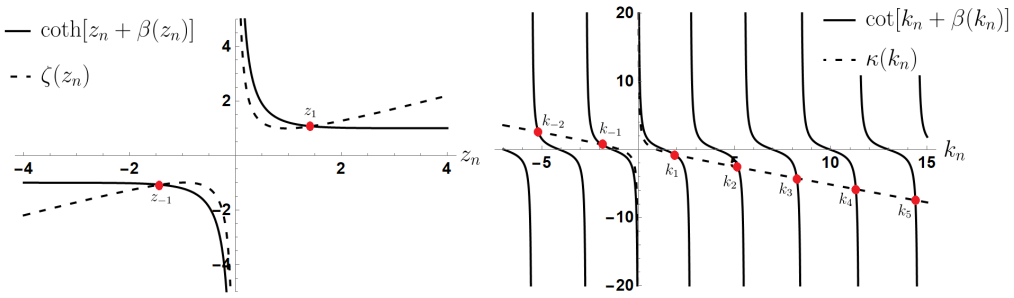


(a) Solutions for $z_n$ real. (b) Solutions for $z_n = ik_n$.

**Figure 3.8.** First solutions of the transcendental equation for: (a) $z_n$ being a real number and, (b) $z_n = ik_n$ being a pure imaginary number.

The supersymmetric partner of $\hat{H}_0^2$ is,

$$\hat{H}_1^2 = -\frac{d^2}{dx^2} + k_y'^2 + 2\,k_\mu^2\,\sec^2\left(k_\mu\,x+\gamma\right),$$

with energies $\bar{\epsilon}_n'^2 = k_y^2 - \xi - z_n^2$. The spinor components depend on the value of $z_n$, which can be a real number or a pure imaginary number, $z_n = ik_n$. In both cases we have that,

$$\phi_n^{(A)}(x) = \sinh\left[z_n\,x+\beta(z_n)\right], \quad \text{or} \quad \phi_n^{(A)}(x) = \sin\left[k_n\,x+\beta(z_n)\right],$$

and the spinor components are given by

$$\phi_n^{(A,1)}(x) = -\frac{1}{\sqrt{\bar{\epsilon}_n'^2 - \bar{\epsilon}_\mu'^2}}\left(\frac{d\,\phi_n^{(A)}(x)}{dx} - W(x)\,\phi_n^{(A)}(x)\right),$$

$$\phi_n^{(B,1)}(x) = -\frac{i}{\bar{\epsilon}_n'}\left(\frac{d\,\phi_n^{(A,1)}(x)}{dx} - \omega_1(x)\,\phi_n^{(A,1)}(x)\right),$$

where,

$$\omega_1(x) = \frac{\nu_1'(x)}{\nu_1(x)}.$$

The different values of $z_n$ are obtained by solving either the transcendental equation (3.56) for $z_n$ being a real number,

$$\coth\left[z_n+\beta(z_n)\right] = \zeta(z_n) = \frac{z_n^2 + k_\mu^2\,\sec^2\left(k_\mu+\gamma\right) - k_\mu\,\omega_1(1)\tan\left(k_\mu+\gamma\right)}{z_n\,\omega_1(1) - z_n\,k_\mu\,\tan\left(k_\mu+\gamma\right)},$$

| | $z_n$ | $\beta(z_n)$ | $\bar{E}'_n = \sqrt{k_y^2 - z_n^2 - \xi}$ | $A$ |
|---|---|---|---|---|
| $z_1$ | 1.4230 | 0.2504 | 1.6766 | 3.06449 |
| | $k_n$ | $\beta(k_n)$ | $\bar{\epsilon}'_n = \sqrt{k_y^2 + k_n^2 - \xi}$ | $A$ |
| $k_1$ | 1.8850 | 0.3142 | 2.8964 | - |
| $k_2$ | 5.1867 | 0.7295 | 5.6336 | 1.0267 |
| $k_3$ | 8.2349 | 0.9571 | 8.5235 | 1.0292 |
| $k_4$ | 11.2999 | 1.0965 | 11.5119 | 1.0210 |
| $k_5$ | 14.3868 | 1.1875 | 14.5539 | 1.0148 |
| $k_6$ | 17.4890 | 1.2505 | 17.6268 | 1.0109 |

**Table 3.3.** First solutions of the transcendental equations, and some parameters that depend on $z_n$ ($\beta(z_n)$, the energy and the normalization constant $A$). We are denoting by $\bar{E}'_n$ the energy expression that depends on $z_n$ and by $\bar{\epsilon}'_n$ the energy expression that depends on $k_n$. The explicit expression for $\beta(z_n)$ is given in equation (3.64) and for $\beta(k_n)$ in equation (3.66).

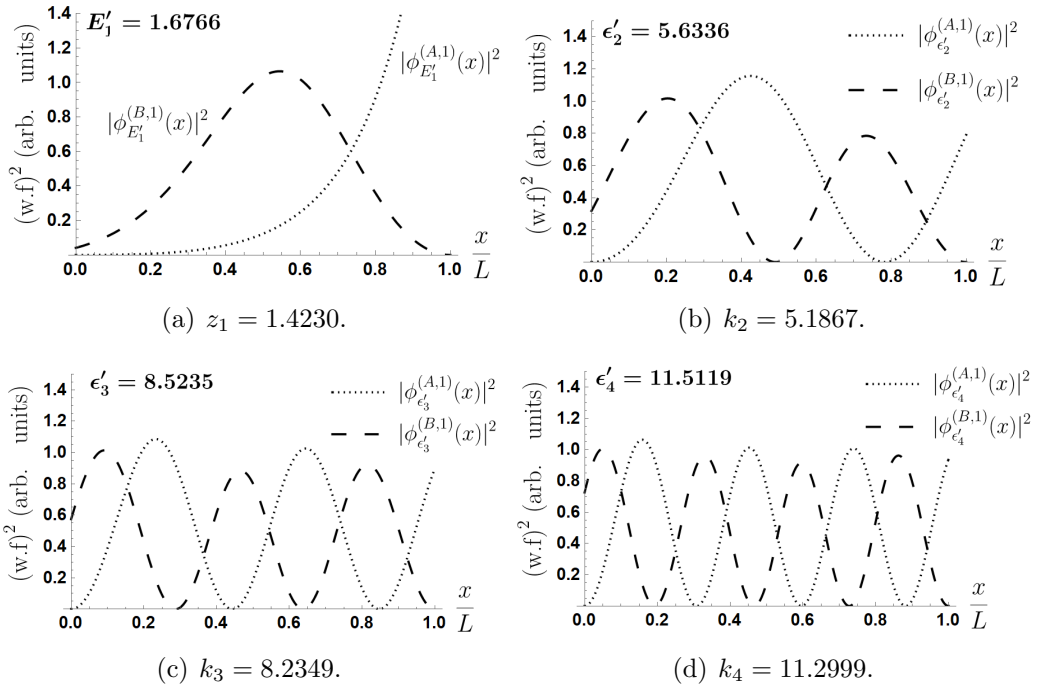


(a) $z_1 = 1.4230$. (b) $k_2 = 5.1867$.

(c) $k_3 = 8.2349$. (d) $k_4 = 11.2999$.

**Figure 3.9.** Modulus square of the entries $\phi_n^{(A,1)}(x)$ and $\phi_n^{(B,1)}(x)$ of the normalized spinor for the first four values of $z_n$. In (a) the lower spinor component at $x = 0$ is not null, $\phi_n^{(B,1)}(0) = 0.0415$. The parameters we are using are $\gamma = \frac{2}{5}\pi$, $\delta = -\frac{2}{5}\pi$, $k_\mu = -\frac{3}{5}\pi$ and $\sqrt{k_y^2 - \xi} = 0.7\pi$.

with $\beta(z_n)$ given by (3.64), and the transcendental equation (3.58) for $z_n = ik_n$ a pure imaginary number,

$$\cot\,[k_n + \beta(k_n)] = \kappa(k_n) = \frac{-k_n^2 + k_\mu^2\,\sec^2\,(k_\mu + \gamma) - k_\mu\,\omega_1\,(1)\tan\,(k_\mu + \gamma)}{k_n\,\omega_1\,(1) - k_n\,k_\mu\,\tan\,(k_\mu + \gamma)},$$

with $\beta(k_n)$ given by (3.66). In Table 3.3 and Figure 3.8 we show the first values of $z_n$ and $k_n$ and the energies associated with them. We will use the notation $\bar{E}_n'$ for the energies of the Dirac Hamiltonian with real values of $z_n$ and $\bar{\epsilon}_n'$ for the energies for imaginary values of $z_n$.

The normalization constants $A$ that we are using satisfy

$$A = \int_0^1 \left( |\phi_n^{(A,1)}(x)|^2 + |\phi_n^{(B,1)}(x)|^2 \right) dx.$$

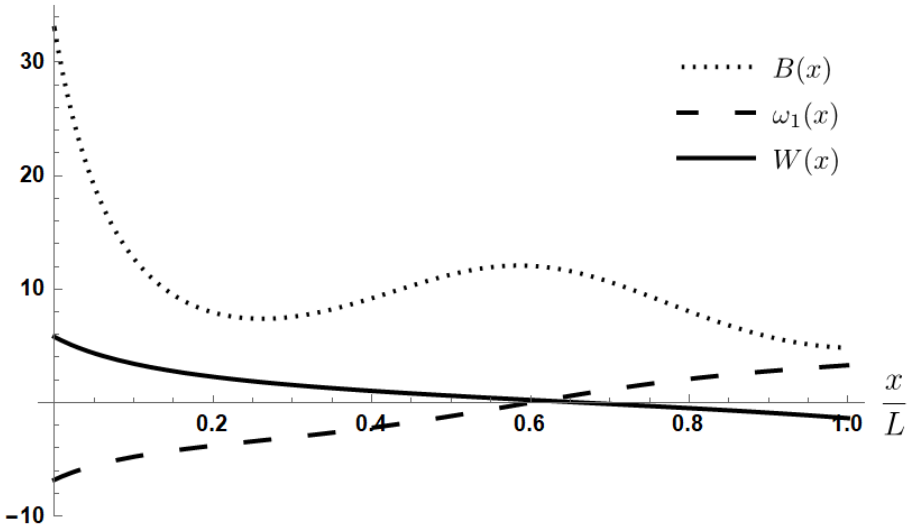


**Figure 3.10.** Magnetic field $B(x)$, function $\omega_1(x)$ and the superpotential $W(x)$.

We calculate this constant numerically for each value of $z_n$, which is reported in Table 3.3. The parameters $k_1 = 1.8850$ and $k_\mu = -1.8850$ have the same absolute value but different sign. Therefore, $\vec{\epsilon}_1'$ and $\vec{\epsilon}_\mu'$ are the same, and the components of the spinor are undeterminate for $k_1$. For the other values of $z_n$ this problem disappears. In Figure 3.9 we show plots of the square of the components of spinor for $z_1$ and for the first three positive values of $k_n$.

As we have already seen in the previous examples, the magnetic field is the derivative of the function $\omega_1(x)$,

$$\mathbf{B}(x) = \frac{d\,\omega_1(x)}{dx}\,\hat{e}_z.$$

In Figure 3.10 we have plotted the corresponding magnetic field, the function $\omega_1(x)$ as well as the superpotential $W(x)$. Compared to the previous examples, this time the magnetic field has no divergences.

# Conclusions

In this thesis we studied solutions to the Dirac equation for zigzag graphene nanoribbons starting from solutions that did not consider an applied magnetic field, we arrive to solutions with an applied non-uniform magnetic fields using the first-order supersymmetric quantum mechanics. We have used as well the SUSY technique to obtain new Schrödinger equations that satisfy the zigzag boundary conditions and we found the expressions of the Dirac Hamiltonians and their spinors for graphene nanoribbons with magnetic field. We studied the values that the parameters of the solutions must have in order that the solutions and the magnetic fields are regular.

In Chapter 3 we used a first-order SUSY transformation for three different purposes. We first used the SUSY transformation to know the expression of the Dirac Hamiltonian associated to the Schrödinger equation (3.1). Then, we used the first-order SUSY to find the supersymmetric partner of the Hamiltonian of equation (3.1). We found that these transformations had superpotential with similar expressions but different meanings. The first SUSY transformation gave solutions to the Dirac equation with zigzag boundary conditions and magnetic field, starting from the solutions to the Dirac equation that Brey and Fertig found in their article [22] without magnetic fields. The second transformation gave us two new Schrödinger equations that share the energy spectrum of equation (3.1) but have associated truncated Pöschl-Teller potentials. If we study the energy spectrum for each transformation, we will notice some differences. The spectrum of the first transformation is the square root of the spectrum of (3.1), while the energy spectrum of the second transformation becomes the spectrum of (3.1) except perhaps for the ground state.

The third SUSY transformation appeared until Section 3.2. With this transformation we obtained the expressions for the Dirac Hamiltonians associated to the Schrödinger equations (3.29) and (3.30) with truncated Pöschl-Teller potentials. The results we obtained were more complicated than in the first two SUSY transformations. In the former cases we just had to solve two transcendental equations, one for the real values of $z_n$ and the other for values of $z_n$ being a pure imaginary number. However, in the last case we had to solve four transcendental equations: one to know which values of the parameters give a nodeless seed solution, another one to fulfill the condition $\phi_n^{(A,1)}(0) = 0$ and two additional ones to obtain the real and pure imaginary values of $z_n$. Then, in Section 3.1 and 3.2 we obtained solutions to several Dirac equations describing a zigzag graphene nanoribbon in different magnetic fields. The spectrum of each Dirac Hamiltonian cannot be expressed by a single algebraic equation but we gave the transcendental equations that can be solved numerically to find it. In each Section we presented some examples for different situations of interest.

As a future work, we could compare our results with the numerical approximations that the tight-binding model gives for zigzag graphene nanoribbons in the magnetic fields that we have found in equations (3.13) and (3.14). We also want to extend the application of the SUSY transformation to graphene nanoribbons with armchair edges. To conclude, we propose as well to study graphene nanoribbons in the pseudo-magnetic fields produced by mechanical deformations.

# Bibliography

[1] P. Wallace. The band theory of graphite. *Physical Review*, 71:622–634, 1947.

[2] K.S. Novoselov, A.K. Geim, S. Morozov, D. Jiang, Y. Zhang, S.V. Dubonos, I. Grigorieva, and A. Firsov. Electric field effect in atomically thin carbon films. *Science*, 306:666–669, 2004.

[3] Nobel Foundation. The Nobel prize in physics 2010. https://www.nobelprize.org/prizes/physics/2010/summary/, 2010.

[4] A. Balandin. Thermal properties of graphene and nanostructured carbon materials. *Nature Materials*, 10:569–581, 2011.

[5] H. Chen, M. Müller, K. Gilmore, G. Wallace, and D. Li. Mechanically strong, electrically conductive, and biocompatible graphene paper. *Advanced Materials*, 20:3557–3561, 2008.

[6] E. Secor, B. Ahn, T. Gao, J. Lewis, and M. Hersam. Rapid and versatile photonic annealing of graphene inks for flexible printed electronics. *Advanced Materials*, 27:6683–6688, 2015.

[7] D.J. Fernandez C. and N. Fernández-García. Higher-order supersymmetric quantum mechanics. In *AIP Conference Proceedings*, volume 744, pages 236–273, 2004.

[8] F. Cooper, A. Khare, and U. Sukhatme. *Supersymmetry in quantum mechanics*. World Scientific, 2001.

[9] G. Junker. *Supersymmetric methods in quantum, statistical and solid state physics*. IOP Publishing Bristol, 2019.

[10] V. Matveev and M. Salle. Darboux transformations and solitons. *Springer–Verlag*, 1991.

[11] C. Lee, X. Wei, J. Kysar, and J. Hone. Measurement of the elastic properties and intrinsic strength of monolayer graphene. *Science*, 321:385–388, 2008.

[12] S. Das Sarma, S. Adam, E. Hwang, and E. Rossi. Electronic transport in two dimensional graphene. *Reviews of Modern Physics*, 83:407–470, 2011.

[13] Y. Tan, Y. Zhang, K. Bolotin, Y. Zhao, S. Adam, E. Hwang, S. Das Sarma, H. Stormer, and P. Kim. Measurement of scattering rate and minimum conductivity in graphene. *Physical Review Letters*, 99:246803, 2007.

[14] F. Chen, J. Xia, D. Ferry, and N. Tao. Dielectric screening enhanced performance in graphene FET. *Nano Letters*, 9:2571–2574, 2009.

[15] P. Edward, D. Alfonso, and A. Vijayaraghavan. *An introduction to graphene and carbon nanotubes*. CRC Press Taylor & Francis, 2017.

[16] A. Castro Neto, F. Guinea, N. Peres, K. Novoselov, and A. Geim. The electronic properties of graphene. *Review of Modern Physics*, 81:109–162, 2009.

[17] T. Ando. Theory of electronic states and transport in carbon nanotubes. *Journal of the Physical Society of Japan*, 74:777–817, 2005.

[18] D. Debaprasad and H. Rahaman. *Carbon nanotube and graphene nanoribbon interconnects*. CRC Press Taylor & Francis, 2015.

[19] S. Iijima and T. Ichihashi. Single-shell carbon nanotubes of 1-nm diameter. *Nature*, 363:603–605, 1993.

[20] D. Bethune, C. Kiang, M. De Vries, G. Gorman, R. Savoy, J. Vazquez, and R. Beyers. Cobalt-catalysed growth of carbon nanotubes with single-atomic-layer walls. *Nature*, 363:605–607, 1993.

[21] R. Saito, G. Dresselhaus, and M.S. Dresselhaus. *Physical properties of carbon nanotubes*. Imperial College Press, 1998.

[22] L. Brey and H. Fertig. Electronic states of graphene nanoribbons studied with the Dirac equation. *Physical Review B*, 73:235411, 2006.

[23] L. Brey and H. Fertig. Edge states and the quantized Hall effect in graphene. *Physical Review B*, 73:195408, 2006.

[24] B. Midya and D.J. Fernandez C. Dirac electron in graphene under supersymmetry generated magnetic fields. *Journal of Physics A*, 47:285302, 2014.

[25] M. Castillo-Celeita and D.J. Fernandez C. Dirac electron in graphene with magnetic fields arising from first-order intertwining operators. *Journal of Physics A*, 53:035302, 2020.

[26] P. Dirac. *The principles of Quantum Mechanics*. Oxford Clarendon Press, fourth edition, 1958.

[27] L. Infeld and T. Hull. The factorization method. *Reviews of Modern Physics*, 23:21–68, 1951.

[28] B. Mielnik and O. Rosas. Factorization: little or great algorithm? *Journal of Physics A*, 37:10007–10035, 2004.

[29] B. Mielnik. Factorization method and new potentials with the oscillator spectrum. *Journal of Mathematical Physics*, 25:3387–3389, 1984.

[30] D.J. Fernandez C. *Trends in supersymmetric quantum mechanics. In: Kuru, Ş. and Negro, J. and Nieto, L. (eds) Integrability, supersymmetry and coherent states*. CRM Series in Mathematical Physics. Springer, 2019.

[31] A. Gangopadhyaya, J. Mallow, and C. Rasinariu. *Supersymmetric Quantum Mechanics: An introduction*. World Scientific, Second edition, 2018.

[32] D.J. Fernandez C. Supersymmetric Quantum Mechanics. *AIP Conference Proceedings*, 1287:3–36, 2010.

[33] A. Schulze-Halberg and B. Roy. Darboux partners of pseudoscalar Dirac potentials associated with exceptional orthogonal polynomials. *Annals of Physics*, 349:159–170, 2014.

[34] A. Contreras-Astorga and A. Schulze-Halberg. The confluent supersymmetry algorithm for Dirac equations with pseudoscalar potentials. *Journal of Mathematical Physics*, 55:103506, 2014.

[35] G. Junker. Supersymmetric Dirac Hamiltonians in (1+1) dimensions revisited. *The European Physical Journal Plus*, 135:464, 2020.

[36] S. D. Kuru, J. Negro, and L. Nieto. Exact analytic solutions for a Dirac electron moving in graphene under magnetic fields. *Journal of Physics Condensed Matter*, 21:455305, 2009.

[37] Y. Concha, A. Huet, A. Raya, and D. Valenzuela. Supersymmetric quantum electronic states in graphene under uniaxial strain. *Materials Research Express*, 5:065607, 2018.

[38] G. Pöschl and E. Teller. Bemerkungen zur quantenmechanik des anharmonischen oszillators. *Zeitschrift für Physik*, 83:143–151, 1933.

[39] A. Contreras-Astorga and D.J. Fernandez C. Supersymmetric partners of the trigonometric Pöschl–Teller potentials. *Journal of Physics A*, 41:475303, 2008.

[40] S. Flügge. *Practical quantum mechanics*. Springer, Second edition, 1994.